Report No. 00.235

Dated: 31 May 1963

FINAL REPORT

"COMPARATIVE EVALUATION OF THERMAL PROTECTIVE MATERIALS FOR SPACE SUIT ASSEMBLIES"

CONTRACT NAS 9-1163

31 MAY 1963

SUBMITTED BY
ASTRONAUTICS DIVISION
CHANCE VOUGHT CORPORATION
P. O. Box 6267 . Dallas 22, Texas

TO

NATIONAL AERONAUTICS AND SPACE ADMINISTRATION

Prepared By:	Checked By:	Approved By:
D. M. Latham	G. B. Whisenhunt	W. C. Trent
Power & Environment	Power & Environment	Manager, Power & Environment
J. D. Welsh		V. G. Polovkas
Power & Environment		Project Engineer, R&D Programs

TABLE OF CONTENTS

LIST OF FIGURES

LIST OF TABLES

LIST OF SYMBOLS

Letter Symbols

BTU	British thermal unit. Unit of heat (= 778 FT-LB)
CFM	Gas flow rate. Cubic feet per minute
E	Radiation constant. (BTU/HR-Ft^2)
F	Geometric form factor
^oF	Temperature, degrees Fahrenheit
Ft^2	Area, square feet
H	Radiation intensity. (watts/cm^2 - micron)
HR	Time, hours
HT-1	DuPont high temperature nylon fabric with aluminized coating on one surface
I	Incident effective radiation. (BTU/HR-Ft^2)
IBM	International Business Machines computer
LB	Pound(s), Unit of mass and weight (force)
N_p	Insulation specific performance. (BTU-LB/HR-Ft^2-^oR)
NRC-2	National Research Corporation aluminized-mylar super insulation
psia	Pressure. Pounds per square inch absolute
Q	Heat flow rate per unit area. (BTU/HR-Ft^2)
^oR	Temperature, degrees Rankine
RH	Gas relative humidity
RPM	Angular velocity, revolutions per minute
SES	Vought Astronautics Space Environment Simulator
ΔT	Temperature difference, ^oF or ^oR
U	Insulation thermal effectiveness. (BTU/HR-Ft^2-^oR)
UV	Ultraviolet portion of electromagnetic-wave spectrum. For solar radiation, UV $\leq$ 380 $m\mu$
W	Weight, pounds

Greek Letters

α	Alpha. Surface absorbtivity for radiation; angle between the point surface normal and a line from the point to the radiation source
γ	Gamma. Angle from a plane containing the sub-solar point on the lunar surface and the longitunidal axis of a cylinder on the lunar surface. The cylinder logitunidal axis is perpendicular to the lunar surface and γ is measured about this axis.
ϵ	Epsilon. Surface emissivity for radiation.
θ	Theta. Angle from sub-solar point for earth or lunar orbit
λ	Lambda. Wavelength for radiation
μ	Mu. Wavelength for radiation expressed as microns or milli-microns ($m\mu$)
π	Pi. Ratio of circumference of any circle to its diameter. (= 3.1416)
ρ	Rho. Reflectivity for radiation
σ	Sigma. Stefan-Boltzmann constant (BTU/HR-Ft^2-$^oR^4$)

ϕ Phi. Angle of solar inclination to a lunar surface normal

Subscripts

e	earth
ea	earth albedo
m	lunar
ma	lunar albedo
s	solar
ses	space envrionment simulator

1.0 SUMMARY

A test program was completed to evaluate the insulation effectiveness and space environment compatibility of 24 Government furnished space suit thermal coverall materials. The samples were selected and tests conducted to determine the following:

a. Optimum number of layers (thickness) of an extra-vehicular space suit thermal coverall garment.

b. Effect of exposure of the materials to a simulated space environment.

c. Optimum cover and inner layer materials.

d. Effect of different coverall construction techniques.

e. Effect of dust accumulation on the outer layer.

f. Data on temperatures and heat flow suitable for calculation of performance of the various materials..

Samples of the various insulating materials, approximately 14" x 14", were tested under hard vacuum in the Vought Astronautics Space Environment Simulator to obtain temperature and heat flow data during exposure to both hot and cold environments. Steady state heat gain from the simulated solar flux ranged from 0.10 to 23.8 BTU/HR-Ft^2 for the 24 samples. Steady state heat loss to the simulated cold of deep space was from 0.091 to 17.65 BTU/HR-Ft^2. The time required for stabilization with a step change from the steady state hot to the steady state cold condition varied from 10 to 120 minutes for the various samples.

Deterioration of materials due to exposure to the ultraviolet (UV) of the simulated solar source and to the vacuum-thermal effects was confined principally to the cover layers. Samples with HT-1 covers (DuPont high temperature nylon, aluminized on one side) showed almost no effects from exposure while samples with NRC-2 covers (National Research Corp. Super-insulation) experienced considerable damage. Damage included discoloring, cracking, curling, tearing.

Three possible thermal environments for extra-vehicular missions, earth orbit, lunar orbit, and lunar surface - were analyzed to determine the maximum and minimum radiation intensities to local point and to the entire circular surface of a cylindrical model of a thermal coverall. These analyses were used with test data from seven representative test samples to predict thermal equilibrium conditions for each type of mission. Predicted surface temperatures were between 230°F (sample 17, lunar orbit, maximum radiation) and -120°F (sample 17, lunar orbit or lunar surface, minimum radiation). Predicted equilibrium heat flows were between + 11.08 BTU/HR-Ft^2 into the sample (sample 21, lunar orbit, maximum radiation) and -17.55 BTU/HR-Ft^2 out of the sample (sample 21, lunar orbit or lunar surface minimum radiation). Sample 15 showed the smallest ranges in heat flow (approximately 1 BTU/HR-Ft^2) for each of the three missions.

A limited comparison was made between sample 3 (HT-1 cover / 7 layers NRC-2) and sample 26 (David Clark pressure suit) for a typical 1/2 hour extra-vehicular mission in a circular equatorial orbit at an altitude of 100 miles. The analysis showed that this extra-vehicular mission possibly can be accomplished with the David Clark suit (no coverall) without undue discomfort to the astronaut if the mission is limited to the earth shadow.

It was concluded from the results of the test and analysis that the final choice of a coverall material should be made from those samples having an HT-1 cover and approximately 7 inner layers separated by dacron spacers. It was also concluded that of all the samples tested the four most suitable in the order of preference are:

Sample	Material
15	HT-1 / 7 layers aluminum - polypropylene laminate with dacron spacers.
19	HT-1 / 7 layers aluminum - mylar laminate with dacron spacers
12	HT-1 / 7 layers aluminum-mylar-aluminum film with dacron spacers
3,4 or 11	HT-1 / 7 layers NRC-2 with dacron spacers

Coverall seams should be kept to a minimum and where seams must be used a velcro seam is a better choice than a sewn seam.

Recommended areas for additional study include further investigation to evaluate in detail the effects of foreign materials on the coverall surface layers and determination of the effects on insulation effectiveness of the astronaut's movements. It is further recommended that before any extra-vehicular mission is undertaken without coverall protection a thorough investigation should be made of the thermal protection problem.

2.0 INTRODUCTION

Adequate thermal protection for an astronaut performing extra-vehicular operations is a requirement of manned space programs. Current full-pressure suits do not provide adequate protection for all extremes of thermal environments.

An insulated coverall garment worn over the full-pressure suit will provide the required thermal protection from natural thermal environments for all extra-vehicular space missions. The feasibility of the insulated coverall concept for thermal protection was proven through tests conducted by Vought Astronautics Division, Ling-Temco-Vought, Inc., under NASA Contract NAS 9-461. While these tests did prove concept feasibility, additional tests and analysis were required to select the most satisfactory material for coverall construction.

Under NASA Contract NAS9-1163, Vought Astronautics has evaluated the insulation effectiveness and material environment compatibility of 24 Government furnished space suit thermal coverall materials. The NASA technical monitor of this program has been Mr. Gil Freedman of the Crew Systems Division, Manned Spacecraft Center, Houston, Texas. The results of this test program and analysis are presented in this report to permit selection by NASA of the most satisfactory material for coverall construction.

3.0 TEST PROGRAM

3.1 Objective

The over-all objective of the test program described herein was to evaluate the insulation effectiveness and material compatibility of 24 samples of Government furnished space suit thermal coverall materials. The specific objectives of the program were to evaluate these insulation samples to determine:

(1) Optimum number of inner layers (radiation shields).
(2) Deterioration of materials from the simulated space environmental conditions.
(3) Radiation properties of cover layers.
(4) Insulation effectiveness of different inner layer materials.
(5) Insulation effectiveness of pressure suit materials.
(6) Influence of dust on the cover layer on insulation effectiveness.
(7) Insulation effectiveness of materials with different seam construction techniques.
(8) Insulation effectiveness of materials using cover layers other than HT-1 and/or different methods of joining inner layers and spacer layers.
(9) Insulation effectiveness of all materials using HT-1 covers and the same number of inner layers.

These objectives were achieved by thermal testing of the sample materials in a simulated space environment. Each sample was tested in the Vought Astronautics Space Environment Simulator by determining the heat flow through the sample during exposure to hot and cold environments. Temperature and heat flow data were obtained for transient and steady state conditions.

3.2 Test Articles

A detailed description of each sample tested is given in Table 1. Test samples consisted of layers of various insulating materials approximately 14" x 14" and held together by single loops of teflon coated fiberglass thread (Dodge Fibers Corporation, Fluorglas 12T-04-020) at the corners. A sample was defined as made up of an "outer layer" or "cover" facing the energy source, "inner layers" away from the energy source, and "spacer layers" used to separate adjacent inner layers from each other. No spacer layer was used to separate the cover or outer layer from the first inner layer.

3.3 Test Equipment

3.3.1 Space Environment Simulator

The Vought Astronautics Space Environment Simulator (SES) simulated space conditions of solar radiation, cold of deep space, and high vacuum. A chamber pressure of 1×10^{-7} to 6×10^{-8} mm Hg was maintained throughout the tests. Pumping was provided by a mechanical ballast pump, an oil ejector pump and three oil diffusion pumps.

The inside walls of the simulator were maintained at -310°F during all tests. The chamber walls were cooled by liquid nitrogen.

Nine Mercury-Xenon high pressure direct current arc lamps simulated solar radiation. Solar heat flux at the target plane was calibrated before and after the test program for each of the six specimen positions. Power supplied to the lamps was monitored during calibration and during all tests. Lamp power readings were used to correct base line flux data to the conditions existing when the steady state heat flow data was recorded. The variation from high value to low value for the total flux on each of the six specimen positions did not exceed 21% for any test run.

The spectral energy distribution of the Mercury-Xenon lamps is shown in Table 2.

3.3.2 Backing Plates

A constant temperature heat sink/source was provided by backing plates through which constant temperature water was circulated. The backing plates, known commercially as Dean Panelcoils, consisted of two 0.06 inch aluminum sheets welded together, one of which was flat (front side) and the other embossed to form a flow channel (back side). A view of the three backing plates as mounted in the Space Environment Simulator for this test is shown in Figure 1. The heat flow transducers used to measure heat flow through insulation samples were attached to the front side of the backing plates. The backing plates measured 12" high by 23" long.

As shown in Figure 1, the backing plates were attached directly to a rectangular frame (aluminum angle stock) which was supported by the chamber motion gimbal. The frame was attached to the motion gimbal by thin wall tubing and micarta blocks. The exposed framework and the back side of the backing plates were insulated with a sheet fiberglass type insulation covered by approximately 25 layers of NRC-2 super insulation.

3.3.3 Water System

Artesian water at a constant temperature of approximately 94.7°F flowed to the backing plates to maintain a constant temperature heat sink/source during all testing.

Water flow of approximately six pounds per minute through the series connected backing plates maintained each plate at essentially the same temperature; i.e., the water temperature rise or drop through the backing plates was very nearly zero throughout the test. Calculated values of water temperature rise or drop also showed near zero values. Copper tubing of nominal 1/4-inch diameter carried the water to and from the backing plates. Flexible tubing at the point of joining the copper tubing to the backing plates permitted rotation of the backing plates, without disrupting water flow. All copper tubing inside the Space Environment Simulator was insulated with sheet fiberglass and approximately 25 layers of NRC-2 super insulation.

A schematic of the over-all test setup is shown in Figure 2.

3.4 Instrumentation

3.4.1 Samples

The surface temperature indication for each sample was obtained by use of a 40 gauge copper-constantan (Cu-Cn) thermocouple attached to the outside cover. The resistance welded thermocouple beads were flattened to less than two mil thickness to obtain as much contact area as possible between the thermocouple bead and the surface. The attachment of the thermocouple to the surface was made by an epoxy compound (Shell Chemical Company - Epon 828 and DTA). The two electrical leads from the thermocouple bead to the edge of the insulation led out separately to minimize heat flow leaks to any one surface area. Sample number 5 had an additional surface thermocouple which was located near the epoxy attached thermocouple. Aluminum - mylar tape attached the extra thermocouple to the surface. The outside surface thermocouple for sample number 7 was also attached by placing it under aluminum - mylar tape.

Profile temperatures were determined for sample number 7 on the top side of the third, ninth, twelfth, and fifteenth inner layers. The thermocouple installations were identical to those on the surface except that a small quantity of Eastman 910 glue attached each 40 gauge thermocouple to the surface.

Beckman and Whitley T200-3 heat flow transducers measured the heat flow through the insulation samples. These thermopile elements produced a microvolt output directly proportional to the one-dimensional heat flow through the samples. Initial transducer size of 4 1/2" x 4 1/2" x 3/64" was increased to 11 1/4" x 11 7/8" x 3/64" by addition of a "picture frame" made of the same bakelite material as the transducer. This was done to insure one-dimensional heat flow through the actual 2 1/2" x 3 1/8" thermopile area in the center of the transducer. Pittsburg Plate Glass Company's Bondmaster M611 adhesive with CH-1 hardner joined the three 1/64" bakelite sheets of the "picture frame" together and to the T200-3 transducer. A view of the six complete heat flow transducers as installed on the backing plates is seen in Figure 1. An epoxy compound (Shell Epon 828 plus General Mills Versamid 115) joined the heat transducers to the backing plates. A Cu-Cn thermocouple embedded in the thermopile area of each transducer provided the temperature for correction of the raw heat flow data through the use of a calibration curve supplied by the manufacturer.

3.4.2 Backing Plates

The backing plate thermocouples were mounted at six points, two per plate with each on the flat side of the plate directly in line with the center of the thermopile area of the transducers. Again 40 gauge Cu-Cn thermocouples were used. Eastman 910 glue was used to attach each thermocouple to the backing plate. A thin sheet of cigarette paper separated the thermocouple from the metal plate to prevent electrical shorting.

3.4.3 Water System

Two Conax Thermocouple Glands with 20 gauge Cu-Cn wire provided measurements of the water inlet temperature to the backing plates and the

Δ T across the backing plates. Water discharge temperature outside the chamber was determined with a mercury thermometer.

3.4.4 Space Environment Simulator

Twelve Cu-Cn thermocouples installed on the SES walls gave temperature measurements of the simulated cold of deep space. The thermocouples were positioned principally on the West inside wall of the SES directly opposite the insulation samples when oriented for a cold test run.

Heat flux intensity and distribution at the target plane were determined before and after the test program using the heat flow pickups shown in Figures 3 and 4. Each of the small pickups of Figure 3 consisted of two copper plates 3" x 3 5/8" separated by micarta blocks with four thermocouples mounted on each plate. The thermocouples were wired in parallel. Each plate was of identical construction except that the back plate (away from the simulated solar heat) had a small electrical heater attached to the inside surface. Fiberglass insulation filled the void between the two plates. In use these pickups were positioned in the target plane at identical positions to the six heat transducers as mounted on the backing plates. The SES lamps were adjusted to the level of solar intensity and the plate electrical heaters power was increased until back plate temperature reached the same value as front plate temperature. The watts per square inch reading for each pickup at this condition gave base line flux intensity for the actual thermopile areas. Similar data after the test runs provided an estimate of the limits of these measurements when correlated with before and after readings of lamp wattages.

The large pickup (10 7/16" x 11") in Figure 4 was centered in turn at each of the six test positions to determine relative heat flux over each test sample. One hundred identical copper plates (squares) separated by insulation made up this pickup. Each copper plate had an identical thermocouple installed on the back side. The thermocouples from four adjacent squares (plates) were paralleled to read a temperature. By establishing a correlation between the millivolt thermocouple output of the small pickups (Figure 3) with the millivolt output of each four adjacent squares, it was possible to determine heat flux distribution and heat flux mean value for each test position over an approximate area of one square foot. A typical heat flux distribution for a test position is shown in Table 3. The lamp wattages at the time of each run were used to make corrections in base line values of heat flux.

3.4.5 Instrumentation Readout Systems

Temperature readout for the Space Environment Simulator cold wall temperatures was a Brown Multipoint Recorder (-10 to 0 / 10 millivolts).

Millivolt readout for test sample temperatures, backing plate temperatures, transducer temperatures, and heat flows was a digital voltmeter system as shown in Figure 5. This system provided the necessary accuracy for the Beckman and Whitley heat flow transducers when operating at low heat flows.

A consolidated Vacuum Corporation GIC-100 gauge was used to monitor space chamber pressure during all test runs.

3.4.6 Instrumentation Accuracy

Estimated instrumentation accuracies are as follows:

Temperatures - Brown Multipoint Recorder	$\pm$ 3°F
Temperatures - Digital Voltmeter System	$\pm$ 1°F
Heat Flows - Digital Voltmeter System plus B & W Heat Flow Transducers	$\pm$ 4% of recorded value
Space Chamber Pressure - CVC GIC-100 gauge	$\pm$ 15%
Solar Flux - Chance Vought Radiometers	$\pm$ 5% (relative values) $\pm$ 10% (absolute values)

3.5 Test Procedure

3.5.1 Preparation of Test Samples

High lateral heat flow in any test sample could have given an erroneous indication of the apparent thermal conductivity of the sample. This possibility was analyzed to determine the magnitude of the problem and to suggest possible solutions. Analysis of possible heat losses due to edge effects is shown in the Appendix.

Analysis of possible heat loss from edge effects showed no serious results, but it did suggest that heat paths should be eliminated where possible. To do this all inner layers except the layer next to the heat transducer were trimmed to the same size as the transducers, 11 1/4" x 11 7/8". The cover layer and all spacer layers were trimmed along one edge to line up with the inside edge of the transducer. Thus available heat paths from the exposed area of the sample to the areas wrapped around the top, bottom, and outside edges of the backing plate were minimized.

METHOD OF TRIMMING THE SAMPLES IS INDICATED IN THE SKETCH BELOW:

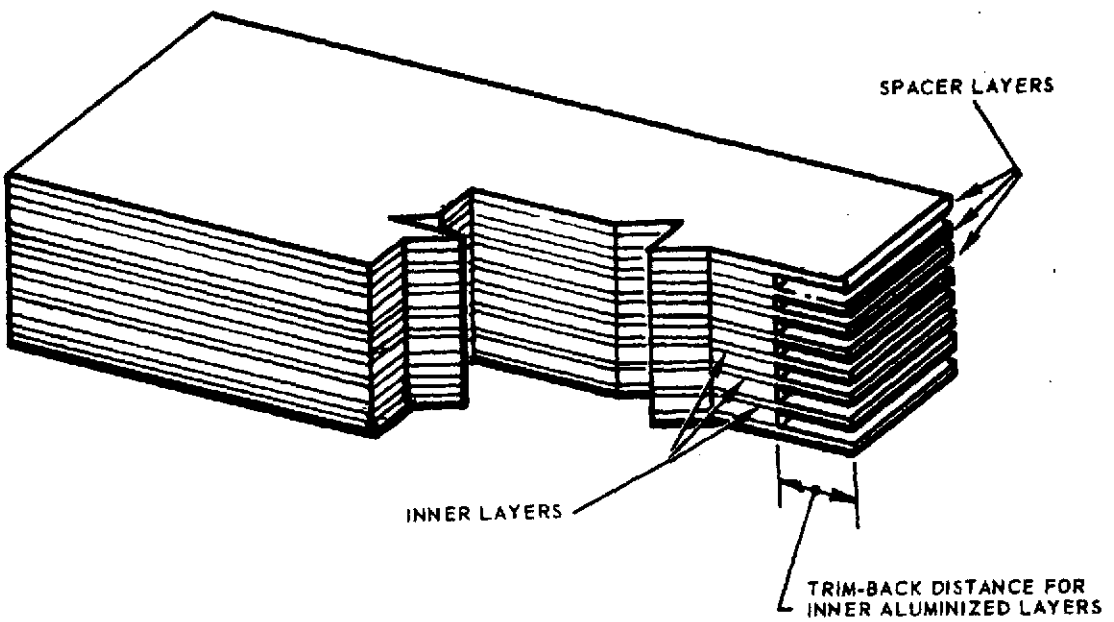

Sample 5 was used to check possible environmental effects of dust on the cover. After rubbing the cover with human hands, basaltic dust was sprinkled over the cover surface. This simulated "moon dust" of mean particle size 10 microns or less was supplied by Jet Propulsion Laboratory, California Institute of Technology.

Each sample was weighed before installation on the backing plates and then weighed again when removed following testing.

3.5.2 Installation of Test Samples

All test samples except number 11 were installed so that the cover, spacer layers, and inside inner layer wrapped around the top, bottom, and outside edges of the backing plates. Sample 11 was inadvertently installed so that the inside and outside edges of the insulation were reversed. The wrap around of each sample was about 1/2 inch with the wrap around area of the sample installed under the insulation covering the back side of the backing plates. A white fiberglass tape was used to

secure the wrap around edges of the samples. Test samples as installed before test runs are shown in Figures 6 through 9. A 1/2" high strip of fiberglass tape was placed between adjacent samples along their common edges as a radiation shield. The sketch below indicates the method of installing test samples.

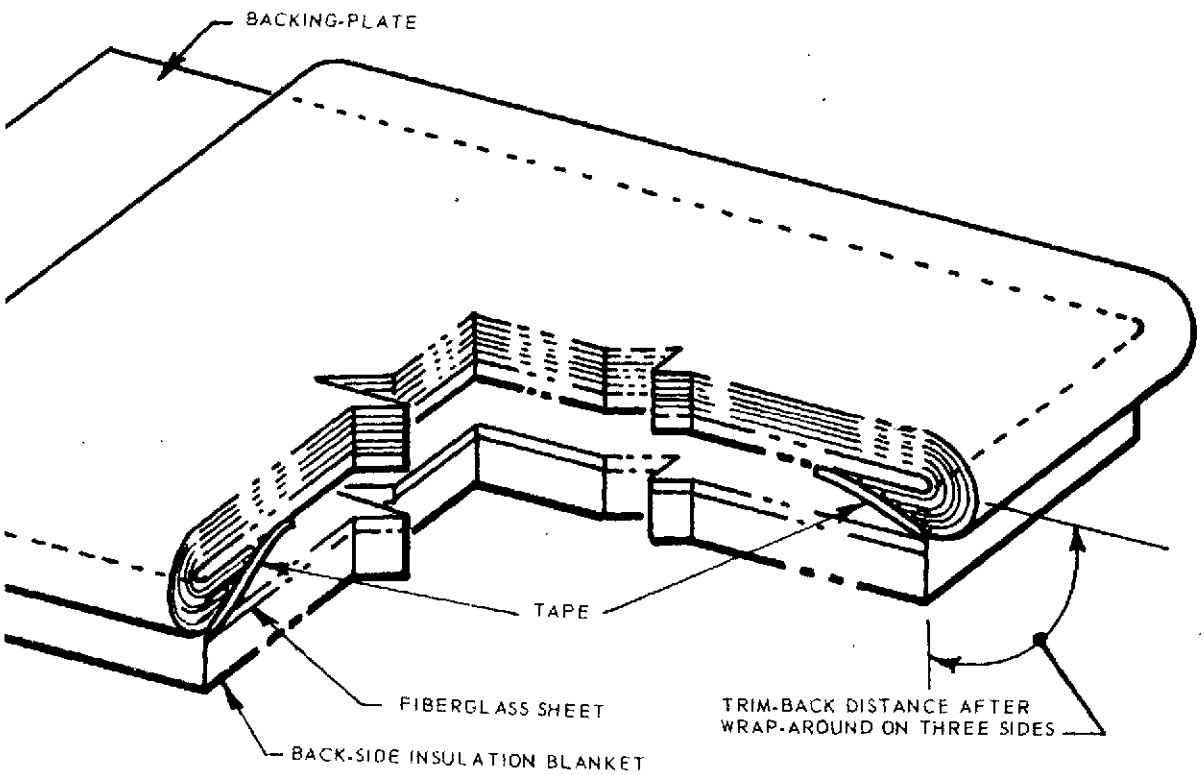

3.5.3 Hot Test Runs

Following a complete check of instrumentation, water flow to the backing plates was started. The pump down and cool down of the chamber required about two hours after which the solar lamps were brought up to power in about 20-30 minutes. After reaching full solar power, steady test conditions were maintained for a minimum period of six hours. The data was recorded throughout the test run and final steady state data was taken at the end of the six hour period.

3.5.4 Transient Test Runs

Each transient run followed immediately after a hot run. Rotation of the samples from facing the solar source to facing the SES cold wall (West) took about 5-10 seconds. A visual check of the new position was made and then the solar source was turned off. Very rapid changes of surface temperatures made it impossible to record these data during the early portion of a transient run. However, heat flow data for each of the six samples was recorded at 30 second intervals. After about 30-60 minutes temperature data was also recorded.

3.5.5 Cold Test Runs

Cold runs covered the period following each transient run until final steady state cold data was recorded. The time lapse from lights off until reading of final cold data was about 2 1/2 - 3 hours. The warm up and return to sea level conditions of the SES took about 10-12 hours after which photographs were made of the samples before removing them from the backing plates (see Figures 10 through 14).

3.5.6 Order of Testing

The testing of 24 samples at a rate of six per day was completed. The first day was generally devoted to optimizing the number of inner layers. Second day tests investigated different inner layers. Third day tests covered the environmental effects of dust on a sample, construction techniques for seams, and other inner layers and cover materials. The fourth day of testing was devoted mainly to samples of full pressure suits with some samples of different construction in the inner layers. Tables 4 through 7 show which samples were run on each test day and the test position of each sample.

3.6 Test Results

Tables 4 through 7 present steady state hot and cold test results. Transient temperature data is presented in Figures 15 through 19 while transient heat flow data is shown in Figures 20 through 23. The specific objectives of the program were to evaluate these insulation samples to determine:

(1) Optimum number of inner layers (radiation shields).
(2) Deterioration of materials from the simulated space environmental conditions.
(3) Radiation properties of cover layers.

(4) Insulation effectiveness of different inner layer materials.
(5) Insulation effectiveness of pressure suit materials.
(6) Influence of dust on the cover layer on insulation effectiveness.
(7) Insulation effectiveness of materials with different seam construction techniques.
(8) Insulation effectiveness of materials using cover layers other than HT-1 and/or different methods of joining inner layers and spacer layers.
(9) Insulation effectiveness of all materials using HT-1 covers and the same number of inner layers.

3.6.1 Optimum Layers

Samples 8, 10, 7 and 6 with 3, 7, 15 and 25 layers of NRC-2 insulation, respectively, offer a comparison of the number of insulating layers versus thermal effectiveness.

Heat flux on these samples during the hot run varied by approximately 21% from the high value to the low value. Surface temperatures varied in approximately the same order as the heat flux intensities.

Measured values of heat flow through these samples were small in magnitude (0.10 to 2.325 BTU/HR-FT^2). Confidence in measured heat flow values is high for two reasons. First, the water temperature drop across the backing plates remained near zero throughout the test which indicates a very low heat flow through the test samples. Second, a comparison of test heat flow and heat flow calibrated using National Research Corporation published data for NRC-2 shows a reasonable correlation. This comparison is shown in the following table.

Sample	Number of Layers	Calculated Q Using Manufacturers' conductivity data and test temperatures	Q Test
8	3	2.105	2.325
10	7	0.524	0.29
7	15	0.555	0.37
6	25	0.286	0.10

In making this comparison, it should be noted that the test samples included spacer layers of dacron between the NRC-2 inner layers. These spacer layers are not included in standard NRC-2 insulation.

Thermal effectiveness ranking of these samples was made by using test data in the following equation:

$$U = \frac{Q_{Test}}{\Delta T_{Test}}$$

where,

U = Over-all thermal effectiveness, BTU/HR-Ft^2 - $^\circ$R

Q_{Test} = Measured heat flux through sample, BTU/HR-Ft^2

$\Delta T_{Test} = T_{Surface} - T_{Back\ plate} \sim ^\circ$R

Figure 24 shows a plot of U versus number of layers for both the hot and cold conditions. As can be seen from the units for U, the best insulation will have the lowest value for U.

Specific performance which incorporates a consideration of the weight penalty as well as the thermal effectiveness is defined by the following equation:

$$N_p = U \times W$$

where the units are:

N_p = Specific performance, BTU-LB/HR-Ft^2 - $^\circ$R

U = Over-all thermal effectiveness, BTU/HR-Ft^2 - $^\circ$R

W = Sample weight after test, pounds

A summary of the specific performance of the various samples is presented in the following table.

Solar source on			No solar input		
Sample	Layers	N_p Hot	Sample	Layers	N_p Cold
6	25	.00001118	8	3	.0000831
10	7	.0001602	10	7	.0000887
7	15	.000236	6	25	.0000978
8	3	.000279	7	15	.0001102

In terms of thermal effectiveness and weight penalty, the best insulation has the lowest value of N_p.

3.6.2 Cover Materials

From the standpoint of covers used, test samples may be divided into the following categories for comparison:

NRC-2 Cover, mylar out - Samples 6, 7, 8, 10

HT-1 Cover - Samples 3, 26, 4, 11, 13, 12, 14, 15, 5, 16, 18, 19, 36

Aluminum - Mylar Cover, aluminum out - Samples 17, 20, 22, 24

Aluminum - Dacron Cover, aluminum out - Sample 25

Rayon Cover - Sample 21

Project Mercury Suit Cover - Sample 27

Heat flux intensity on these samples varied by about 21% from the high to the low value. As shown by Table 2 the spectral distribution of the Space Environment Simulator lamps is such that approximately 36% of the total energy is in the ultraviolet wavelength range. In comparison, the ultraviolet energy in the solar spectrum represents approximately 6% of the total energy.

Damage to the cover materials from exposure to the SES environment is shown in Figures 10 through 14. As was expected from the results of the previous test program (NASA Contract NAS 9-461), the NRC-2 cover samples were extensively damaged. The aluminum - mylar samples with the aluminum surface out were also badly damaged with the exception of sample 17. The rayon cover sample showed some color fading while all other samples showed very little apparent effects from the exposure.

Cover material damage in all cases was attributed to the effect of the ultraviolet radiation on the mylar plastic with secondary damage due to the vacuum and thermal effects.

3.6.3 Surface Radiant Properties

Investigations of surface radiant properties have shown that a low value of solar absorptivity to emissivity ratio, (α_s/ϵ) for the suit coverall outer layer is desirable. This keeps cover surface temperature to a lower value and assures a low value of heat flow into the suit.

In this program, surface radiant properties were examined first by use of Vought Astronautics IBM Routine for calculating total radiant properties from spectral data. This routine calculates total radiation properties from spectral data by determining the mean value of a radiation property for a given spectral energy distribution. Inputs to the routine are: (1) solar wavelength (λ solar) vs. solar total emissive power (H_λ solar), (2) space environment simulator wavelength (λ SES) vs. space environment simulator total emissive power (H_λ SES), (3) sample reflectivity (ρ sample) vs. sample wavelength (λ sample), (4) standard reflectivity (ρ standard) vs. standard wavelength (λ standard), and (5) temperature ($^\circ$R) for black body radiation. The data for ρ sample vs. λ sample was furnished by NASA. Outputs of the routine are absorptivity of the surface to solar radiation (α_s), absorptivity of surface to space environment simulator radiation (α SES), and body emissivity of the surface for a range of temperatures (ϵ vs. $^\circ$R).

Additional investigation of the surface radiant properties of the samples consisted of calculating values of α SES/ϵ using test data inputs. The following equation relates the steady state conditions of heat absorption by the surface, heat radiation from the surface, and heat flow through the surface.

$$\frac{\alpha \, SES}{\epsilon} = \frac{\sigma T^4}{\epsilon} + \frac{Q}{E \epsilon}$$

where:

α SES = absorptivity of the surface to Space Environment Simulator radiation, dimensionless

ϵ = black body emissivity of surface at some temperature, dimensionless

σ = Stefan-Boltzmann constant 0.171×10^{-8} BTU/HR-Ft^2 - $^{\circ}$R

T = surface temperature, $^{\circ}$R

E = heat flux on sample in Space Environment Simulator, BTU/HR-Ft^2

Q = heat flow through sample, hot run, BTU/HR-Ft^2

The value of ϵ for the above equation describing a hot run was assumed to be the same ϵ as that derived from the cold steady run data from the following equation:

$$\epsilon = \frac{Q}{\sigma T^4}$$

where:

ϵ = black body emissivity at some temperature, dimensionless

Q = heat flow through sample, cold run, BTU/HR-Ft^2

T = cold surface temperature, $^{\circ}$R

Examination of sample data for reflectivity versus wave length shows that generally the curve is flat between the wave lengths associated with black body emissivity at cold and hot surface temperatures. This indicates that the assumption of ϵ hot = ϵ cold is generally sound.

All values of $\frac{\alpha \text{ SES}}{\epsilon}$ and ϵ cold derived from test data are presented in Tables 5 through 8. However, some of these values are repeated below for comparison with the IBM derived data.

Sample Cover	IBM		TEST
	αSolar/ϵ	αSES/ϵ	αSES/ϵ
Aluminum-Mylar, Multi Layer Mylar out	.72	.98	$.7\text{-}.95_{200^{\circ}F}$
Aluminum-Mylar, Multi Layer, Mylar out Clean	.76	.98	$.7\text{-}.95_{200^{\circ}F}$
HT-1, Aluminum out	.76	.75	$1.5\text{-}2.3_{300^{\circ}F}$
Aluminum-Mylar with Alodine	.88	1.02	$1.8_{300^{\circ}F}$
Aluminum-Mylar, Multi Layer, Mylar out Dust	$.84_{200^{\circ}F}$	$1.06_{200^{\circ}F}$	Not tested
Aluminum-Mylar, Single Layer Mylar out	$.85_{200^{\circ}F}$	$.87_{200^{\circ}F}$	Not tested

Variations in radiant properties between IBM and TEST values can be attributed to test tolerances in T, E, Q, ρ samples, ρ standard, and to the fact that IBM calculations were based on data obtained in an earth air mass whereas TEST calculations data were obtained in a hard vacuum.

3.6.4 Other Multi-Layers

Investigation of insulation samples in terms of inner layer materials, construction, heat transfer properties, and weight was also completed during the program.

The insulation samples which were evaluated to study the above parameters are summarized in the table below:

Sample	Material	Construction Technique
12	Aluminum-Mylar	Film deposit of aluminum, two sides
13	Gold-Mylar	Film deposit of gold, one side
14	Aluminum-Kodar	Aluminum foil-Kodar laminate
15	Aluninum-Polypropylene	Aluninum foil-Polypropylene laminate
19	Aluminum-Mylar	Aluminum foil-Mylar laminate

Thermal ranking of these samples according to effective "U" (where U is over-all thermal effectiveness as defined in Paragraph 3.6.1) gives the results shown below:

Solar source on			No solar input		
Sample	Material	U hot	Sample	Material	U cold
15	Al-Polypropylene L.	.006	12	Al-Mylar Film	.000402
19	Al-Mylar Laminate	.00736	13	Gold-Mylar Film	.001128
14	Al-Kodar L.	.00745	15	Al-Polypropylene L.	.00151
12	Al-Mylar Film	.00817	19	Al-Mylar Laminate	.00199
13	Gold-Mylar Film	.0106	14	Al-Kodar L.	.001995

As explained in Paragraph 3.6.1 above, insulation samples with lower "U" values indicate better thermal performance.

Performance ranking based on specific performance, N_p (where N_p is the same as is defined in Paragraph 3.6.1) is presented in the following table.

Solar source on			No solar input		
Sample	Material	N_p hot	Sample	Material	N_p cold
12	Al-Mylar Film	.000515	12	Al-Mylar Film	.0000254
15	Al-Polypropylene L.	.000530	13	Gold-Mylar Film	.0000689
13	Gold-Mylar Film	.000648	15	Al-Polypropylene L.	.0001334
19	Al-Mylar Laminate	.000652	19	Al-Mylar Laminate	.0001741
14	Al-Kodar L.	.000808	14	Al-Kodar L.	.000216

Insulation samples showing lower N_p values are better materials from the standpoint of thermal and weight performance.

3.6.5 Suit Samples

Several insulation samples were tested which are typical of the materials used in current full pressure suits. These samples were David Clark Suit (26), Rayon-Polyurethene-Nylon Treco (21), Project Mercury Suit (27), and International Latex Corporation (ILC) Suit (36).

Thermal performance ranking for these samples is indicated below where lower values of "U" indicate better thermal performance.

Solar source on		No solar input	
Sample	U_{hot}	Sample	U_{cold}
ILC	.266	ILC	.0855
David Clark	.32	Rayon Cover	.0919
Rayon Cover	.3365	David Clark	.1036
Mercury	.554	Mercury	.1235

Specific performance ranking of these suit samples are summarized in the following table.

Solar source on		No solar input	
Sample	N_p hot	Sample	N_p cold
ILC	.0294	Rayon Cover	.00882
Rayon Cover	.0323	ILC	.00945
Mercury	.05125	Mercury	.01163
David Clark	.1156	David Clark	.0374

Lower values of "N_p" demonstrate better insulation properties per unit insulation weight.

3.6.6 Environmental Sample

Sample 5 with an HT-1 cover treated with basaltic dust provided test data for evaluating possible thermal effects due to a dust accumulation on the suit such as might be encountered on the lunar surface.

A comparison of sample 5 with sample 4 (HT-1 cover, no dust) shows that the dust produced significant decrease in hot steady state thermal effectiveness. This decrease in hot "U" for sample 5 resulted from a decrease in Q by a factor of 5 and a decrease in ΔT by a factor of 2. The table below shows this comparison:

Solar source on		No solar input	
Sample	U_{hot}	Sample	U_{cold}
4	.0144	4	.001338
5	.00582	5	.00188

A specific performance comparison of sample 5 with sample 4 shows a significant change for hot steady state N_p because of the difference in respective U_{hot} values. This comparison is presented below:

Solar source on		No solar input	
Sample	$N_{p\ hot}$	Sample	$N_{p\ cold}$
4	.0009	4	.0000836
5	.000375	5	.0001209

A final comparison of sample 5 with sample 4 in terms of surface radiant properties can be made for TEST and IBM values of $\frac{\alpha SES}{\epsilon}$.

Sample	IBM $\frac{\alpha SES}{\epsilon}$	TEST $\frac{\alpha SES}{\epsilon}$
4	.75	2.25
5	Not determined	.850

3.6.7 Construction Technique Samples - Seams

Two samples, 16 and 18, were tested to permit investigation of seams on thermal effectiveness. Sample 16 consisted of two separate pieces joined in the middle with a velcro seam, while sample 18 consisted of two separate pieces joined in the middle with a sewn seam using a fold-back technique.

A comparison of thermal effectiveness of these samples and an unsewn sample of identical construction follows:

Solar source on		No solar input	
Sample	U_{hot}	Sample	U_{cold}
3 (unsewn)	.0133	3 (unsewn)	.00273
16 (velcro)	.0227	16 (velcro)	.01632
18 (sewn)	.0746	18 (sewn)	.0325

A similar comparison in terms of specific performance shows these results:

Solar source on		No solar input	
Sample	N_p hot	Sample	N_p cold
3 (unsewn)	.000871	3 (unsewn)	.0001789
16 (velcro)	.00211	16 (velcro)	.001517
18 (sewn)	.00547	18 (sewn)	.00238

3.6.8 Other Samples

Five other samples (17, 20, 22, 24, 25) which differed in some details - cover, inner layers, spacer layers, or construction techniques - from all other samples were tested. The thermal effectiveness of these samples is shown below:

Solar source on		No solar input	
Sample	U_{hot}	Sample	U_{cold}
17 (Al-Mylar, Alodine)	.0121	25 (Al-Dacron, NRC-2)	.001216
25 (Al-Dacron, NRC-2)	.01218	17 (Al-Mylar, Alodine)	.00249
24 (Al-Mylar, Spot)	.01717	22 (Al-Mylar, Tulle)	.002865
20 (H-S)	.0267	24 (Al-Mylar, Spot)	.00366
22 (Al-Mylar, Tulle)	.0559	20 (H-S)	.00481

Specific performance ranking of these five samples follows:

Solar source on		No solar input	
Sample	N_{phot}	Sample	N_{pcold}
17 (Al-Mylar Alodine)	.000542	25	.0001077
25 (Al-Dacron, NRC-2)	.001079	17	.0001117
24 (Al-Mylar, Spot)	.001245	22	.0001431
20 (H-S)	.001918	24	.0002655
22 (Al-Mylar, Tulle)	.002792	20	.000345

3.6.9 HT-1 Cover Samples

For convenience of analysis the U_{hot} and U_{cold} values for all samples having HT-1 covers and the same number of inner layers and spacer layers are shown below.

Solar source on		No solar input	
Sample	U_{hot}	Sample	U_{cold}
5 (Dust on cover)	.00582	12	.000402
15 (Al-Poly Laminate)	.006	13	.001128
19 (Al-Mylar Laminate)	.00736	4	.001338
14 (Al-Kodar Laminate)	.00745	15	.00151
12 (Al-Mylar Film)	.00817	11	.0018
13 (Gold-Mylar Film)	.0106	5	.00188
11 (NRC-2 Control)	.01285	19	.00199
3 (NRC-2 Control)	.0133	14	.001995
4 (NRC-2 Control)	.0144	3	.00273
16 (Velcro Seam)	.0227	16	.01632
18 (Sewn Seam)	.0746	18	.0325

Specific performance ranking of these same samples is given below:

Solar source on		No solar input	
Sample	N_{phot}	Sample	N_{pcold}
5 (Dust on cover)	.000375	12	.0000254
12 (Al-Mylar Film)	.000515	13	.0000689
15 (Al-Poly Laminate)	.000530	4	.0000836
13 (Gold-Mylar Film)	.000648	11	.0001174
19 (Al-Mylar Laminate)	.000652	5	.0001209
14 (Al-Kodar Laminate)	.000808	15	.0001334
11 (NRC-2 Control)	.000839	19	.0001741
3 (NRC-2 Control)	.000871	3	.0001789
4 (NRC-2 Control)	.000900	14	.0002160
16 (Velcro Seam)	.00211	16	.001517
18 (Sewn Seam	.00547	18	.00238

3.6.10 Transient Runs

The transient temperature data for sample surfaces and for the profile sample (7) are shown in Figures 15 through 19. The transient heat flow data for each day's runs are shown in Figures 20 through 23. The backing plate temperatures remained essentially constant throughout any one day's runs.

4.0 ANALYSIS OF SPACE THERMAL ENVIRONMENT

Application of insulation materials to thermal protection of an astronaut performing extra-vehicular operations must include an analysis of the anticipated thermal environments. Of immediate interest in this country's space program are the thermal environments for earth orbit, lunar orbit, and the lunar surface. An analysis to define the environment for each of these conditions is presented in the following paragraphs.

4.1 Earth Orbit

Results of the earth orbit environment analysis are presented in Figures 25 through 27. Incident radiation on a cylinder model was considered from three energy sources: solar, earth radiation, and earth albedo. The cylinder axis was assumed to remain parallel to the earth's surface in an equatorial orbit at a constant altitude of 100 miles. Incident radiation was plotted versus orbit angle which was defined as degrees from the sub-solar point. Source radiation constants used for this case as well as all others are listed below:

Solar Constant	E_s	= 445 BTU/HR-Ft^2
Earth Radiation Constant	E_e	= 69 BTU/HR-Ft^2
Earth Albedo Constant	E_{ea}	= 169 BTU/HR-Ft^2
Lunar Radiation Constant	E_m	= 414 BTU/HR-Ft^2
Lunar Albedo Constant	E_{ma}	= 31 BTU/HR-Ft^2

The first case considered was that of maximum radiation to a point on the surface of a non-rotating cylinder. This condition was examined for the point directly opposite the earth and for the point 180° from this position. Form factors for earth radiation and earth albedo were obtained from reference (1).

In the second case, maximum total radiation to the cylinder was determined by allowing the cylinder to spin slowly about its longitudinal axis. Form factors for earth radiation and earth albedo for this case were obtained from Tables 3 and 22, of reference (3). Examination of the outside coverall temperature in Figure 14 of reference (2) shows that the required speed of rotation is relatively low if the cylinder is considered to be of similar material to the coverall. For this figure, a step change in surface temperature was attained by rotating the model through 180° in about 5 - 10 seconds. The surface temperature changed through 200 °F in 5 minutes which shows a response of 40 °F/minute. Thus, if the cylinder model rotates at 1 RPM, any point will change in temperature by no more than $\leq$ 20 °F since any point on the cylinder will be exposed to a given radiation source for about half of its rotation period. Thus, a rotation speed of 1 - 5 RPM is considered adequate to provide negligible surface temperature variation.

An example showing the method used to calculate a point on the total radiation curve (Figure 30) is shown below.

Conditions: Earth Albedo (E_{ea}) = 168 BTU/HR.Ft^2

Orbit Angle (Θ_s) = 20°

Solution: Form Factor (F) from Table 22, Reference
100 mile altitude = 1.373

Incident Albedo Radiation (I_{ea}) = $E_{ea} F$

$$= (168)(1.373)$$

$$= 73.5 \frac{BTU}{HR.Ft^2}$$

4.2 Lunar Orbit

Lunar orbit analysis results are plotted in Figures 25, 28, and 29 as incident radiation versus orbit angle. A cylindrical model with the longitudinal axis parallel to the lunar surface at a circular orbit altitude of 100 miles was assumed. The radiation sources considered were solar, lunar radiation, and lunar albedo.

Maximum local radiation to a point on the non-rotating cylinder was analyzed for the point directly opposite the lunar surface and with the point 180° from this position. The curve for the 180° point is identical with Figure 25, which is the corresponding case for the earth orbital condition. The form factors for lunar radiation and albedo were obtained from reference (1).

The case for maximum total radiation to the cylinder was analyzed while spinning the cylinder slowly. This again distributed the incident flux over the entire surface and provided negligible variation in the resultant surface temperature. The form factors for lunar radiation and lunar albedo were obtained from reference (3). The calculation procedure was the same as for the corresponding case in earth orbit.

4.3 Lunar Surface

Results of the lunar surface analysis are shown in Figures 30 and 31 as incident radiation versus the angle of the sun's rays from the lunar surface normal. The cylinder model was placed with its longitudinal axis perpendicular to the lunar surface. The radiation sources used were solar radiation, lunar radiation, and lunar albedo.

Maximum local radiation to a point on the cylinder surface was used as the first case. The form factors for all three radiation sources are the same and are equal to the cosine of the angle between the sun's rays and the cylinder surface normal.

Maximum total radiation for a cylinder on the lunar surface was determined with the cylinder spinning slowly. The form factors were identical to the first lunar surface case and division by π was necessary to distribute the flux over the larger area ($I = EF/\pi$).

5.0 APPLICATION OF SUIT MATERIAL TO SPACE THERMAL ENVIRONMENT

Selection of suit materials for various extra-vehicular missions must consider material thermal properties and the mission environment. Several materials representing the range of thermal properties of those materials tested were analysed to show predicted thermal equilibrium conditions at maximum and minimum heat flux for a given orbit or mission. These predicted values would be attained for four hour and 24 hour missions under the assumed conditions. For a 1/2 hour mission the predicted values are conservative, since some suit materials would not have completely stabilized thermally in this time. Two suit materials, David Clark (Sample 26) and HT-1 / 7 layers NRC-2 (Sample 3) were compared in more detail for predicted performances during a typical 1/2 hour mission. Four of the most promising materials were analysed further to determine the most suitable coverall material.

5.1 Predicted Thermal Equilibrium Conditions

Seven samples were chosen for analysis to determine thermal equilibrium conditions. Choice of these samples was made to cover the range of values of α/ϵ, U_{hot}, U_{cold} for the different sample types. Samples 20, 22, 24, and all NRC-2 cover samples were omitted from consideration because of cover deterioration during testing. No consideration was given to sample weight in this analysis.

Assumptions made for the analysis are summarized and discussed below.

$\alpha_{S/\epsilon}$ =	$\frac{\alpha_{SES}}{\epsilon}$ Test	The comparative closeness of $\alpha_{S/\epsilon}$ and $\alpha_{SES/\epsilon}$ shown by IBM analysis is the basis for this assumption.
$\alpha_{e/\epsilon}$ =	1.0	This is predicted surface thermal response to earth or moon radiation.
E_s =	E_{solar} / E_{albedo}	The wavelengths of solar radiation and reflected solar radiation are considered to be the same.
E_e =	E_{earth} or E_{moon}	This is infra-red radiation from the earth or the moon.
Q =	U_{Test} ($T_{surface}$ - T_{inside})	This is predicted unit heat flow through the suit at equilibrium.
ϵ =	ϵ_{Test}	

Suit Model = Spinning Cylinder

T_{inside} = 90°F

Calculations of equilibrium surface temperature and steady state heat flow were obtained by balancing the following equation:

$$T_{surface} = \sqrt[4]{\frac{\alpha S}{\epsilon}\ \frac{E_s}{\sigma} + \frac{\alpha e}{\epsilon}\ \frac{Ee}{\sigma} - \frac{Q}{\epsilon\sigma}}$$

The results of this analysis are presented in Table 8. From this table it can be seen that samples 12 and 19 show the smallest range in Q (heat flow) values from the hot to the cold conditions, whereas samples 27 and 21 show the greatest range in Q values between the hot and the cold conditions.

5.2 Extra-vehicular Mission Without and With Coverall Protection

The degree of thermal protection provided by a coverall garment was determined using data from this test as applied to a typical extra-vehicular mission. The mission selected was a circular, equatorial earth orbit with an altitude of 100 miles and a period of 90 minutes. Extra-vehicular time was assumed to be 30 minutes.

An HT-1 + 7 layers of NRC-2 sample (3) was compared with the David Clark sample (26). Sample (3) represented a coverall material and the David Clark sample represented a pressure suit material. Each sample was considered singly, i.e., for analysis purposes sample thermal properties were examined as if sole thermal protection was provided by this sample.

Assumptions made for this analysis were as follows:

Astronaut Metabolic Heat = 10 BTU/MIN (600 BTU/HR)

Astronaut Perspiration Output = .009667 pounds water per minute (reference (4))

Oxygen pressurization system = 5 CFM of O_2 at 3.5 psia

$T_{in} = 45^{\circ}F$

$T_{out} = 90^{\circ}F$ or $100^{\circ}F$

$RH_{in} = 0\%$

$RH_{out} = 75\%$

Suit Shape = Cylindrical Shell

Suit Area = 30 Ft^2

Spinning Model - No seams in suit materials - Materials transient thermal characteristics were consistent with test data - Material emissivity and apparent thermal conductivity values were equal to test values. Excess heating rate was defined as: Metabolic heat - O_2 sensible cooling - Perspiration cooling + heat flow through suit material.

The excess heating rate versus time curve (Figure 32) shows that suit temperatures incur smaller variations with a coverall than with a pressure suit. Thus, internal coverall temperatures can be controlled as a function of oxygen flow rate versus astronaut activity without regard to environmental extremes. However, if extra-vehicular missions are limited to the earth shadow, a heat leaking pressure suit will aid the flow-rate cooling. The environments considered in determining Figure 32 were solar flux, earth albedo, earth radiation, vehicle albedo, vehicle radiation and deep space.

5.3 Selection of Most Suitable Coverall Materials

The samples considered in the final choice of a most suitable coverall material were limited to those with HT-1 covers. The HT-1 covers proved to be more resistant to deterioration from the simulated solar environment than the others tested.

By inspection of the performance of the seven HT-1 samples analyzed in paragraph 5.1, it was possible to narrow the choice down to four samples. Final selection was based on the following three criteria: (1) minimum heat flow through the sample between maximum and minimum equilibrium surface conditions for typical extra-vehicular missions; (2) heat flow through the sample at maximum equilibrium surface conditions should be as close to zero as possible and (3) a low value of N_p , specific performance, for hot and cold test runs is desired. As shown in Table 9, sample 15 best met these criteria. The low values of heat flow at maximum temperature assure minimum effect on the astronaut's suit conditioning system from the external environment. Low values of N_p indicate good thermal effectiveness per unit weight of insulation. Although these four samples are ranked in order of preference, it is obvious from Table 10 that all four are good choices for a suit coverall material and the differences in predicted performance are small.

6.0 CONCLUSIONS

The insulation effectiveness and materials compatibility were determined for 24 Government furnished space suit thermal coverall materials. The applicability of the test materials to various extra-vehicular missions was evaluated.

Conclusions regarding specific objectives of this program are as follows:

(1) Optimum number of layers - The thermal effectiveness of NRC-2 insulation with dacron spacers varies directly with the number of layers used. Seven layers of NRC-2 with dacron spacers offers the best specific performance.

(2) Deterioration of materials from environmental conditions - The damage is confined primarily to the cover layer and the HT-1 fabric offers the best choice of cover materials.

(3) Other inner layer materials - The aluminum polypropylene sample (15) and the aluminum-mylar film sample (12) show the best thermal effectiveness and specific performance of this group of samples.

(4) Comparison of pressure suit samples - The ILC sample (36) and the rayon cover sample (21) demonstrate the best thermal effectiveness and specific performance. Coverall samples tested are up to 350 times better in terms of thermal effectiveness and specific performance than pressure suit samples.

(5) Environmental effects (dust) on the cover layer - Dust on the cover layer of an HT-1 sample improves thermal effectiveness and specific performance under hot conditions by 1.5 - 2.0. For cold conditions, dust on the cover layer reduces thermal effectiveness and specific performance by 1.5 - 2.0.

(6) Construction techniques (seams) - One piece no-seam construction is desired to minimize heat shorts in a coverall material. In areas where seams must be used, the velcro seam is approximately 1.5 to 3.0 times more effective than the sewn seam.

(7) Other cover layers and other construction methods - With the exception of the aluminum-dacron sample (25), these materials are not suitable for coverall construction because of deterioration.

(8) All HT-1 cover samples with the same number of inner layers - The final choice of a coverall material should be made from this group because the best cover material is used and the seven inner layer construction offers the optimum value in thermal effectiveness with weight penalty.

An extra-vehicular mission of 30 minutes (earth orbit) with only the thermal protection of the pressure suit (David Clark) and with sensible-latent cooling by oxygen circulation can possibly be accomplished without

undue astronaut discomfort if the mission is confined to the earth shadow.

The most suitable coverall materials in the order of preference are:

Sample 1[illegible] - HT-1 + 7 Al-Polypropylene laminate with Dacron Spacers

Sample 19 - HT-1 + 7 Al-Mylar laminate with Dacron Spacers

Sample 12 - HT-1 + 7 Al-Mylar-Al film with Dacron Spacers

Samples 3, 4, or 11 - HT-1 + 7 NRC-2 with Dacron Spacers.

7.0 RECOMMENDATIONS

The results of this test program indicate several areas in which additional investigation should be undertaken. The recommended areas for additional investigation are discussed below.

(1) The surface radiative properties of the HT-1 cover material are changed significantly by the presence of dust. Additional investigations should be made to evaluate in detail the effects of foreign materials on cover material surface radiative properties. This investigation should be completed prior to undertaking extra-vehicular missions on the lunar surface.

(2) The effects of the astronau't mobility, i.e., the movements of his body, on the insulation effectiveness of suit materials and coverall materials should be determined.

(3) The brief analysis of an extra-vehicular mission without coverall protection as presented in paragraph 5.0 of this report indicates that thermal protection afforded by a pressure suit material (David Clark Suit) is marginal. A thorough investigation should be made of this problem before undertaking an extra-vehicular mission without coverall protection.

(4) Complete coverall garments should be checked under simulated extra-vehicular mission conditions. Simulation should include radiation fluxes, cold of deep space, astronaut mobility and movement, variation in radiation flux with orbit angle, astronaut metabolic heat, and full-pressure suit pressurization and ventilation.

LIST OF REFERENCES

1. Yandell, H. W. and Hixon, C. W. "Thermal Radiation Form Factors In Space", AST/E3TM-2, Chance Vought Astronautics, January 1963.

2. Knezek, R. A. and French, R. J., "Final Report Space Suit Thermal Test Program Contract NAS9-461", Chance Vought Astronautics, September 1962.

3. Stevenson, J. A. and Grafton, J. C., "Radiation Heat Transfer Analysis For Space Vehicles," ASD Technical Report 61-119 Part I, United States Air Force, December 1961.

4. Breeze, R. K., "Space Vehicle Environmental Control Requirements Based on Equipment and Physiological Criteria", ASD Technical Report 61-161 Part I, United States Air Force, December 1961.

F I G U R E S

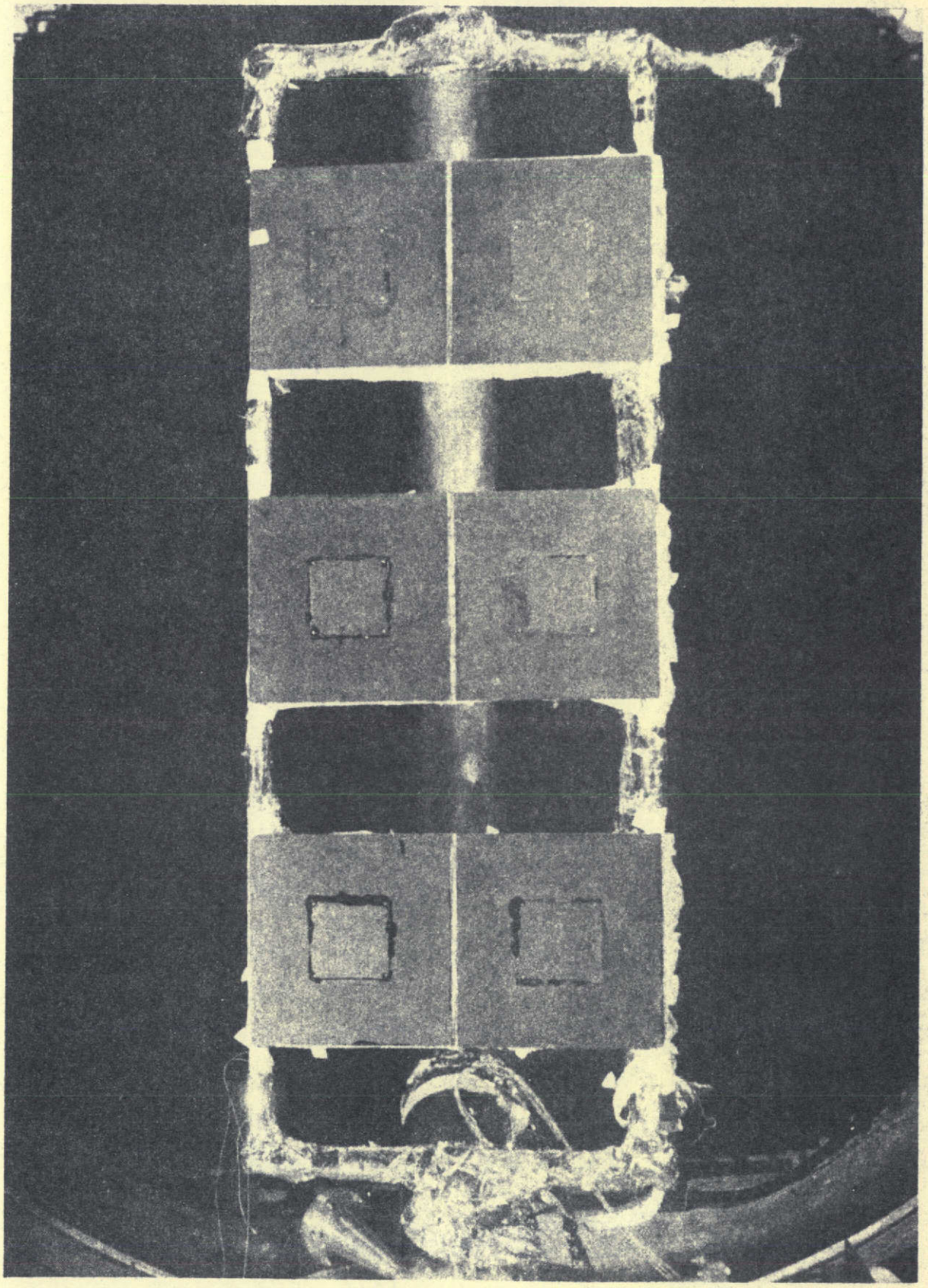

FIGURE 1 BACKING PLATES MOUNTED IN SES

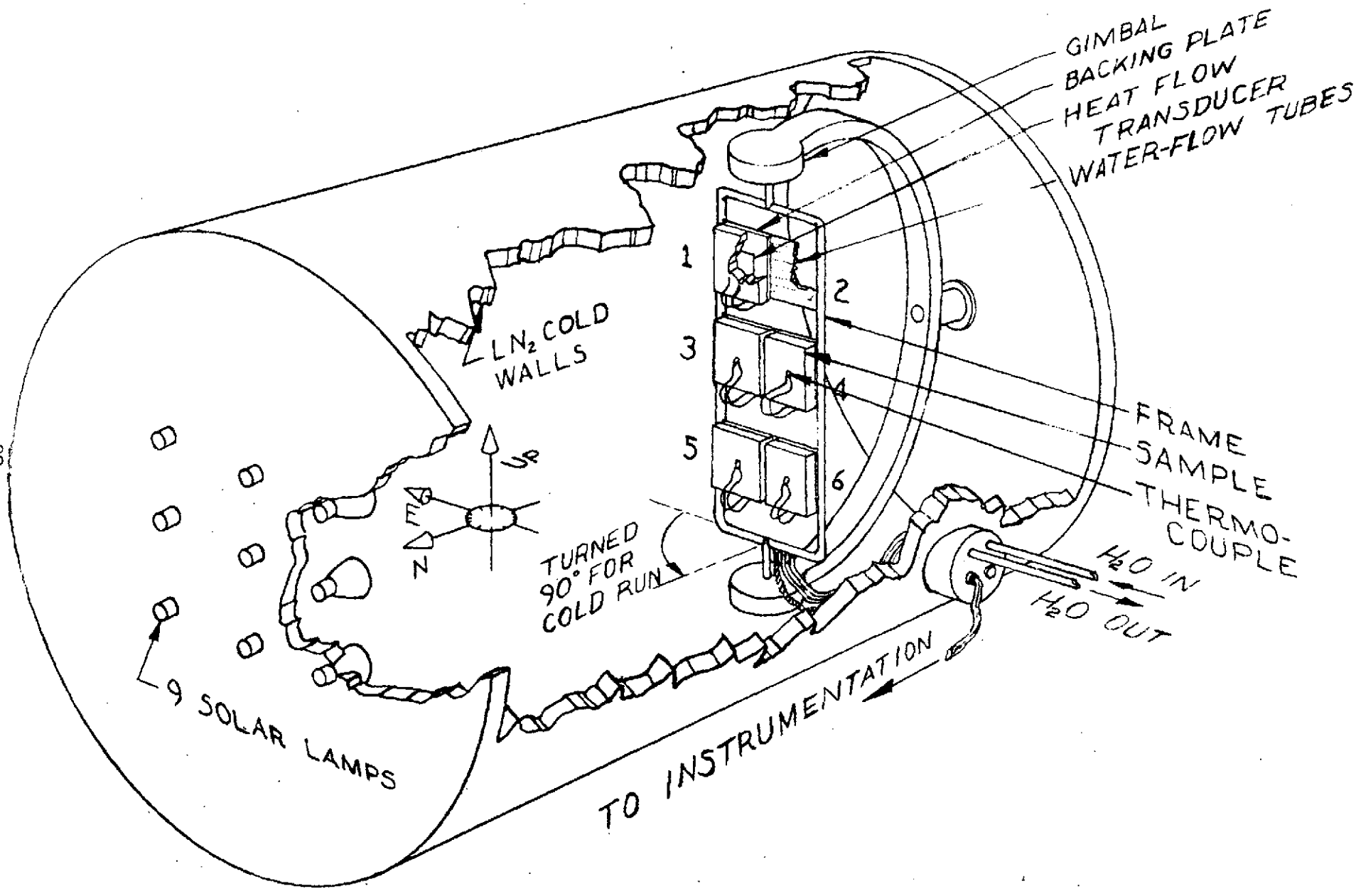

FIGURE 2 TEST SET-UP SCHEMATIC SPACE ENVIRONMENT SIMULATOR

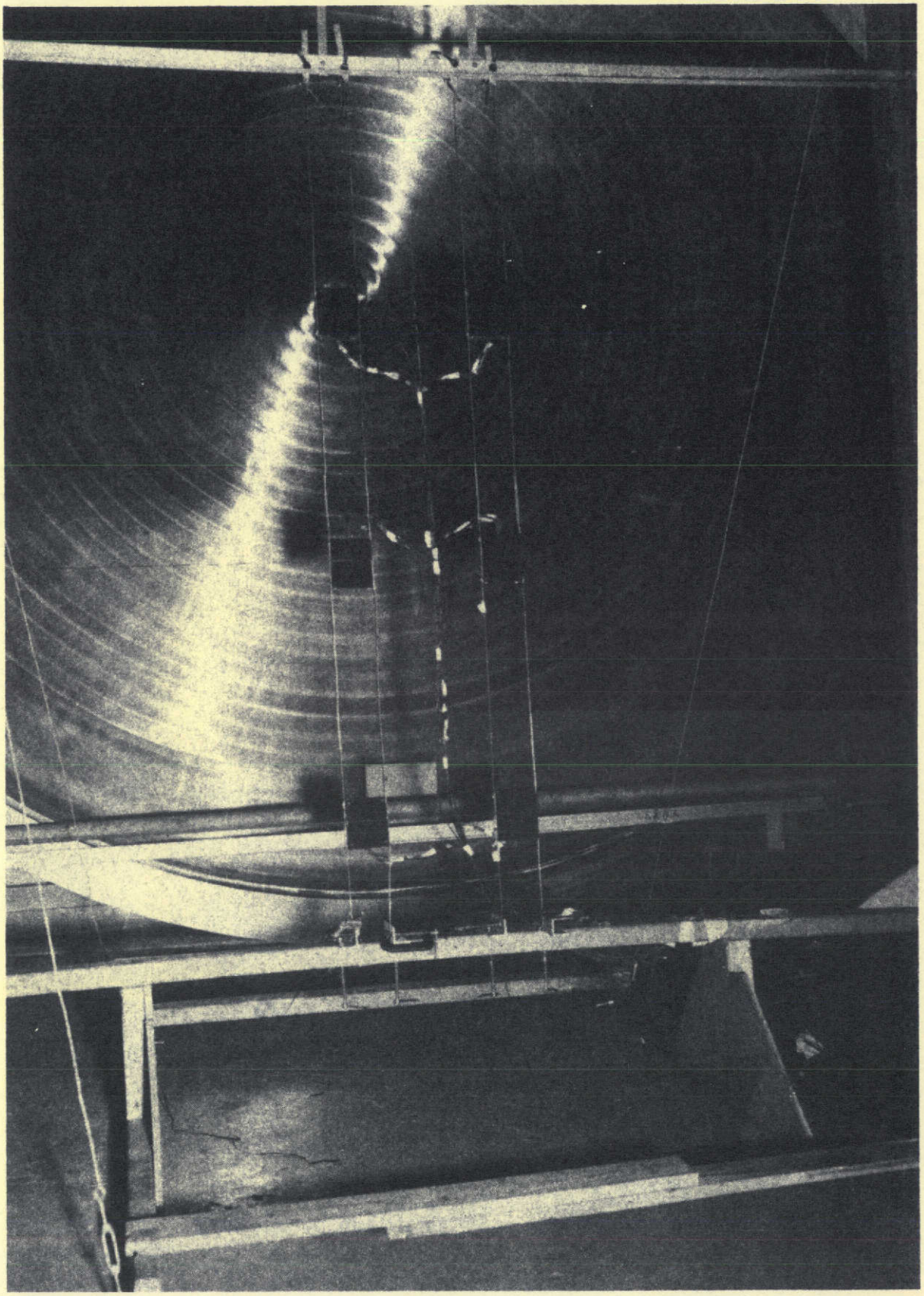

FIGURE 3 CALIBRATION RADIOMETERS, SMALL

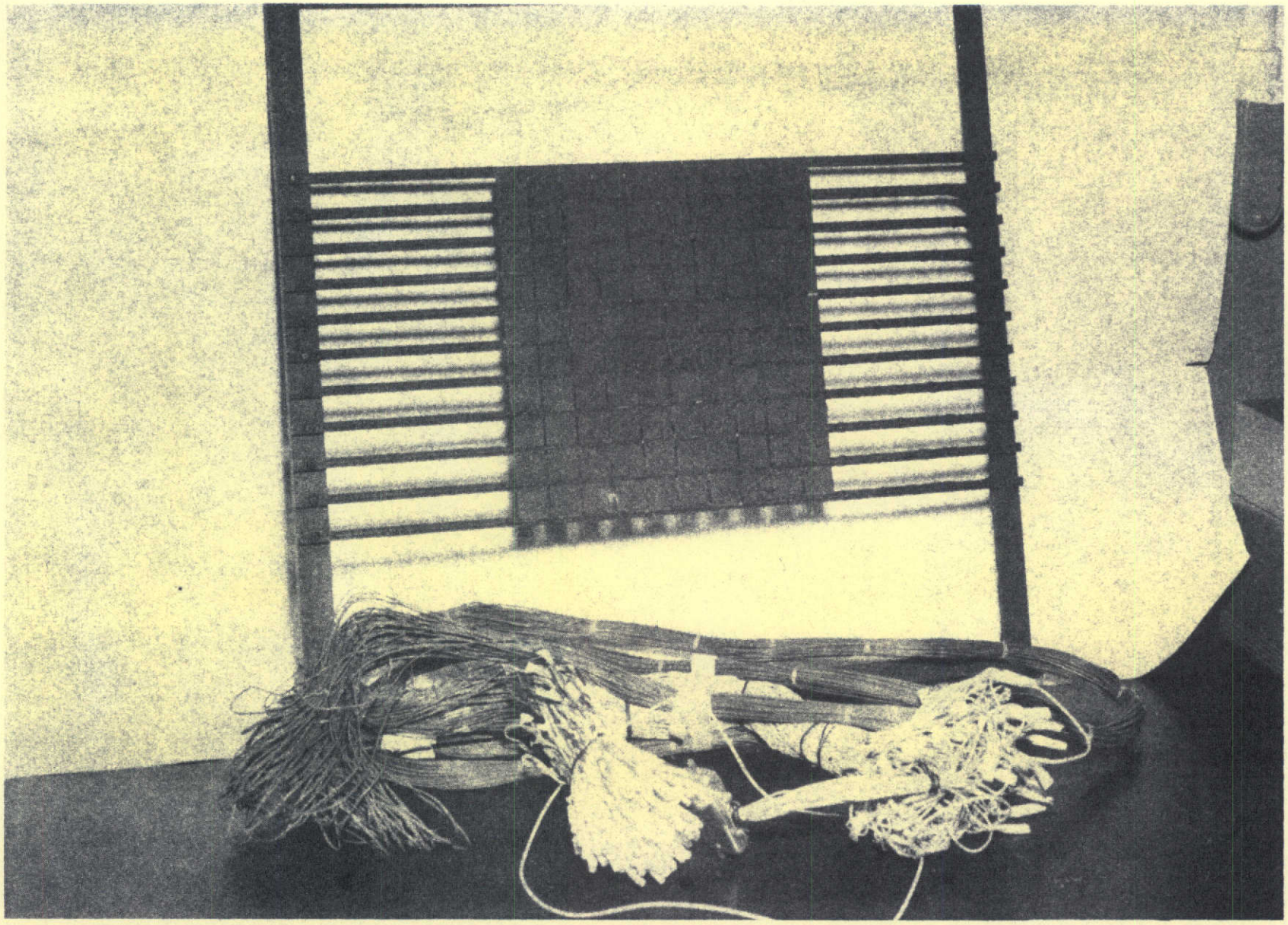

FIGURE 4 CALIBRATION RADIOMETER, LARGE

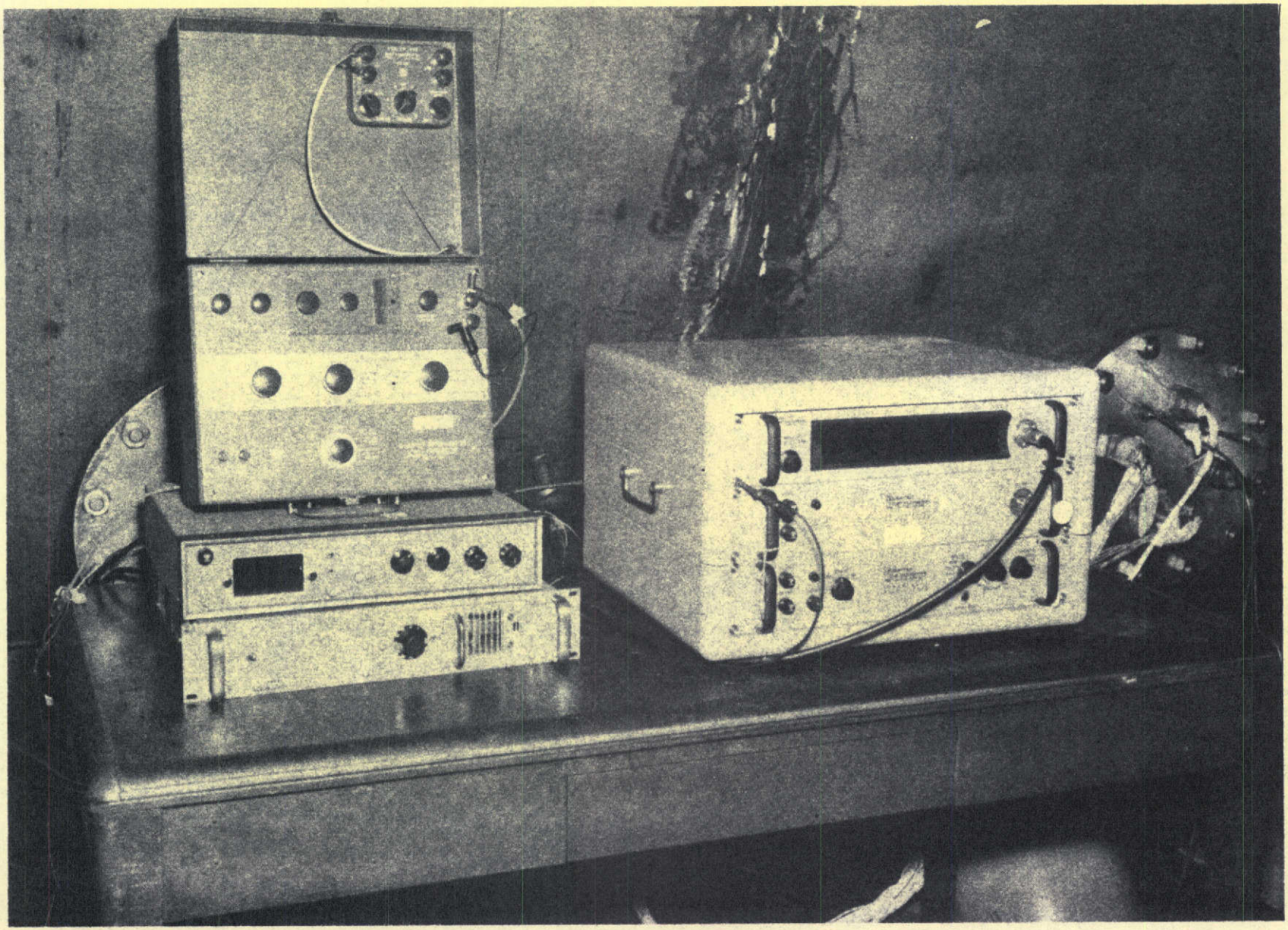

FIGURE 5 DIGITAL VOLTMETER SYSTEM

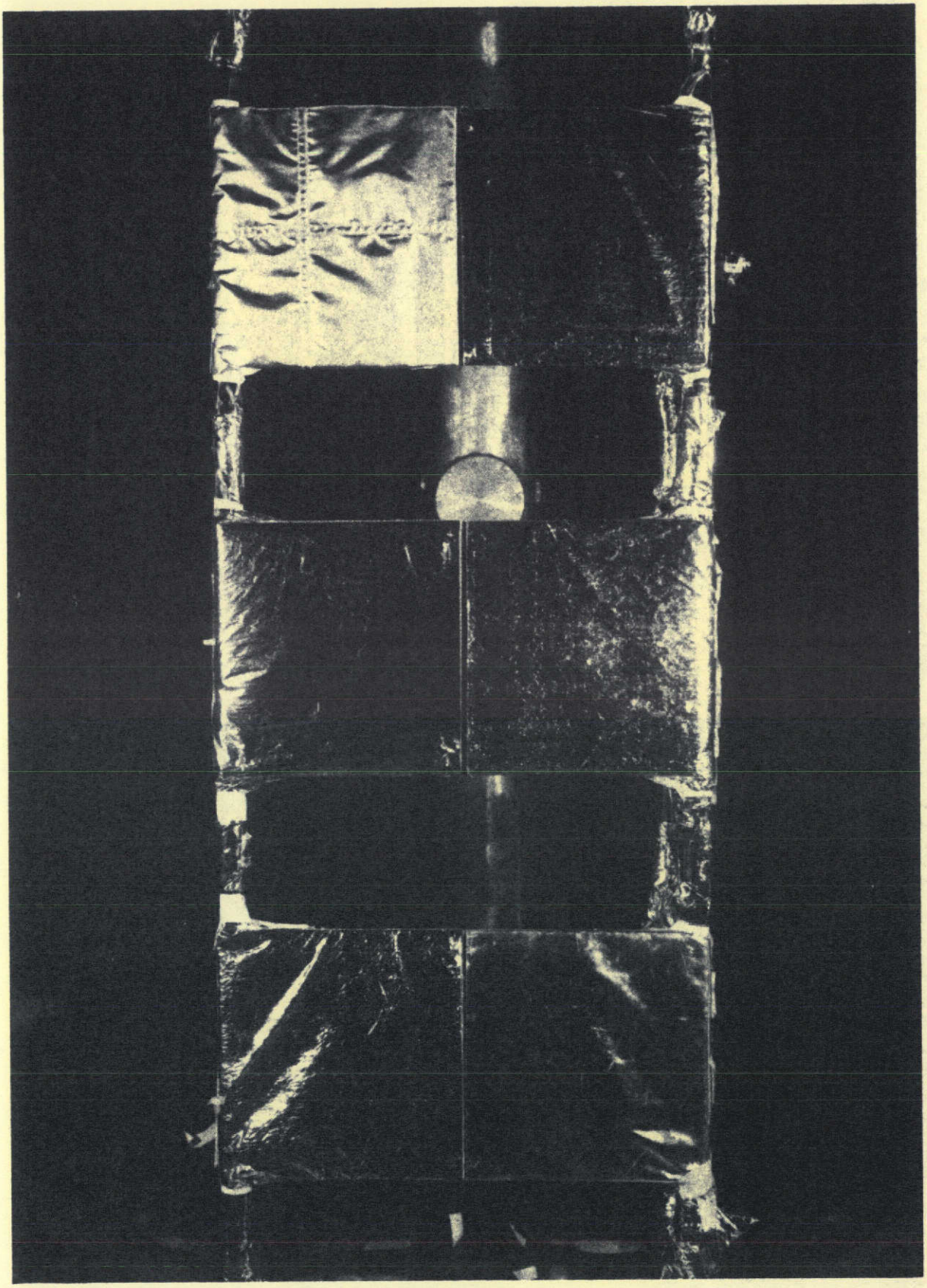

FIGURE 6 SAMPLES BEFORE RUN – FIRST DAY

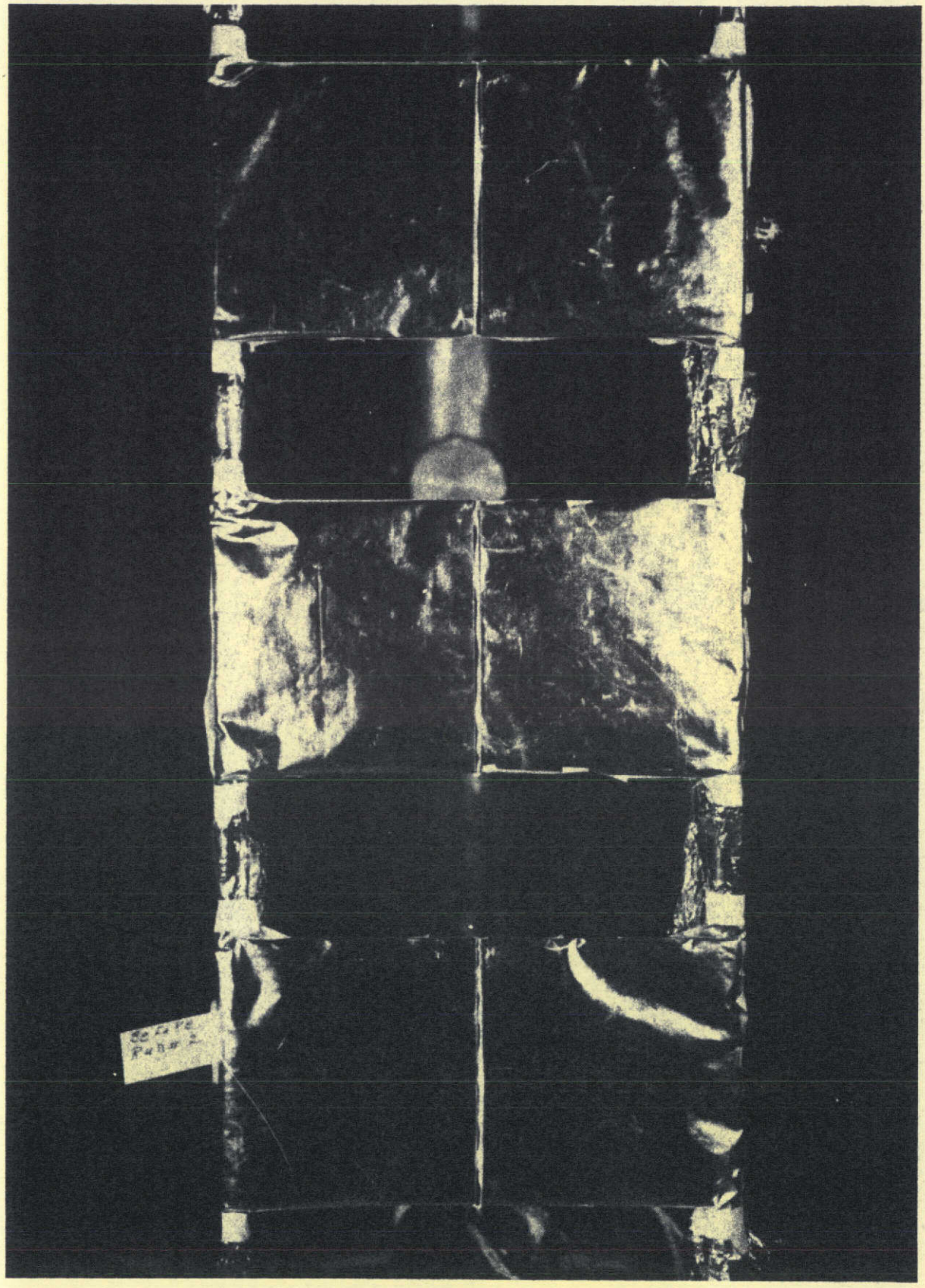

FIGURE 7 SAMPLES BEFORE RUN – SECOND DAY

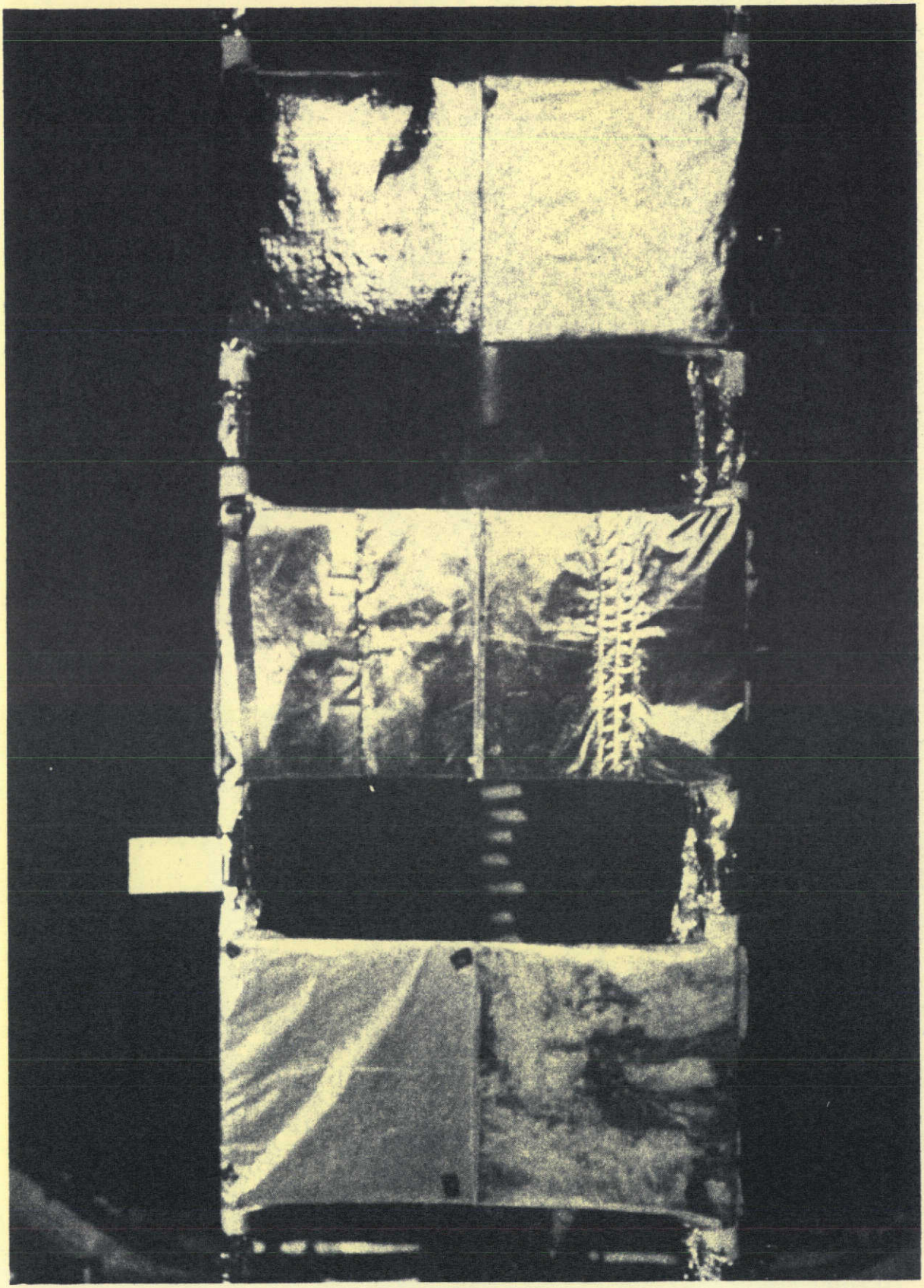

FIGURE 8 SAMPLES BEFORE RUN – THIRD DAY

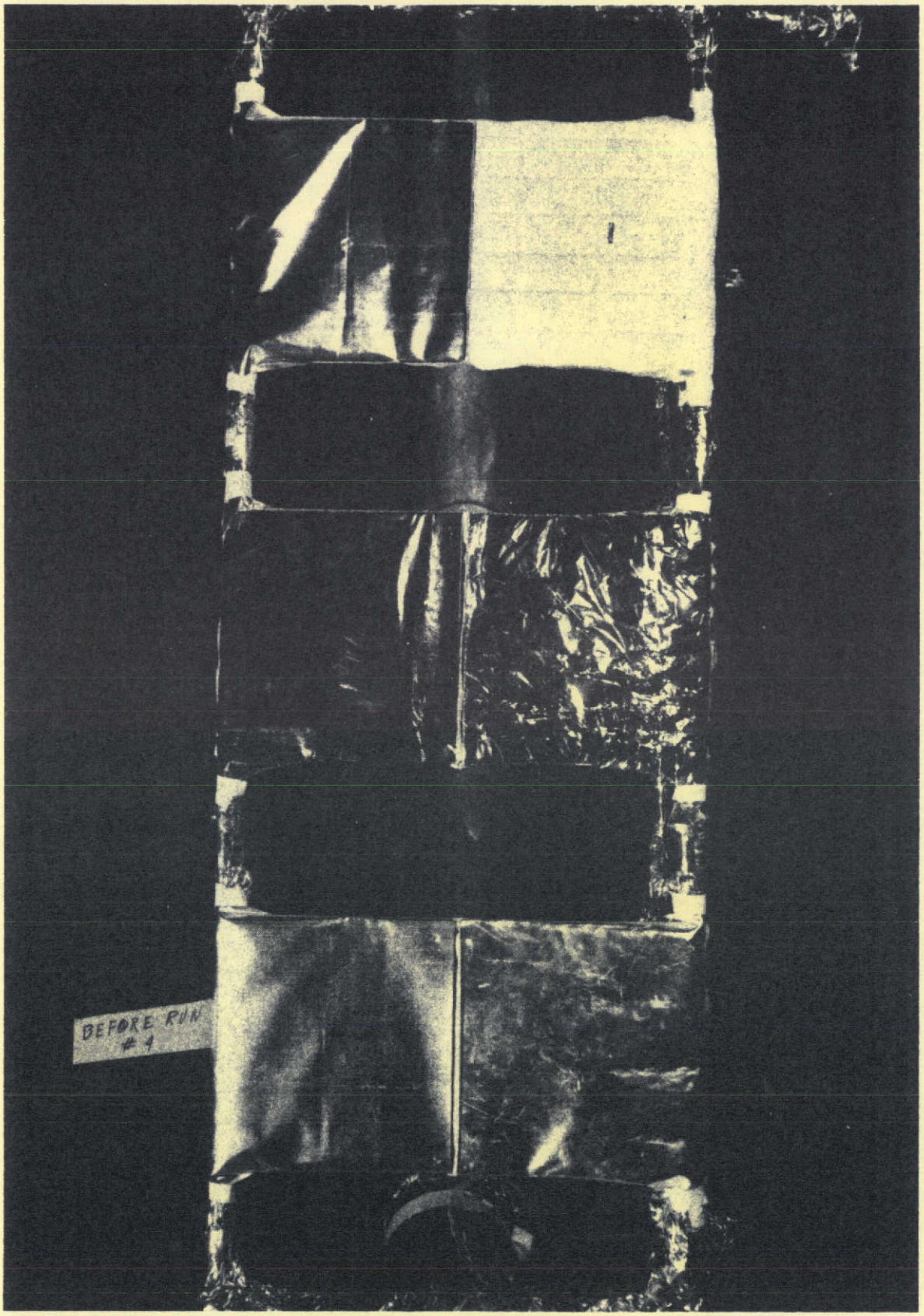

FIGURE 9 SAMPLES BEFORE RUN – FOURTH DAY

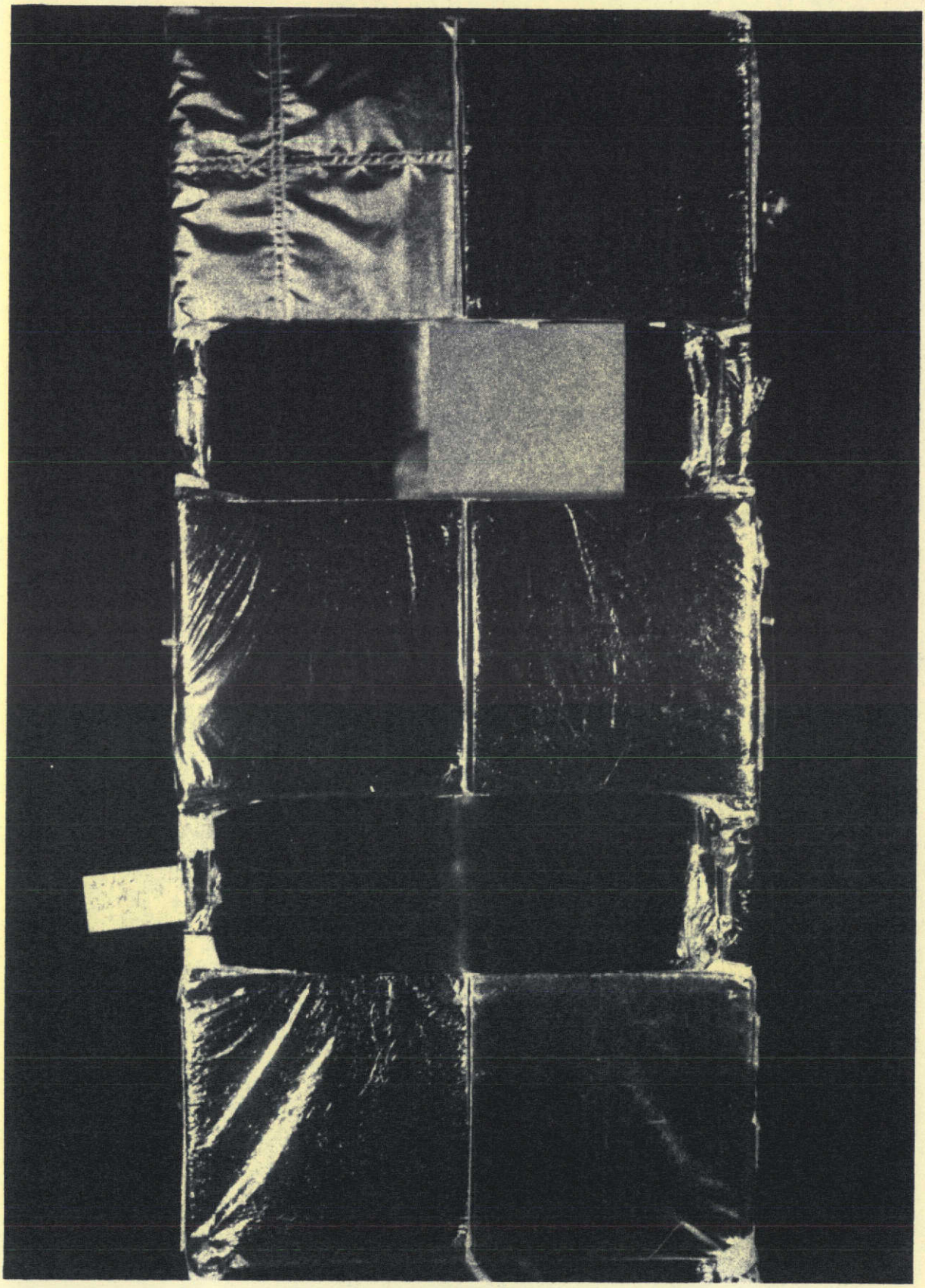

FIGURE 10 SAMPLES AFTER RUN – FIRST DAY

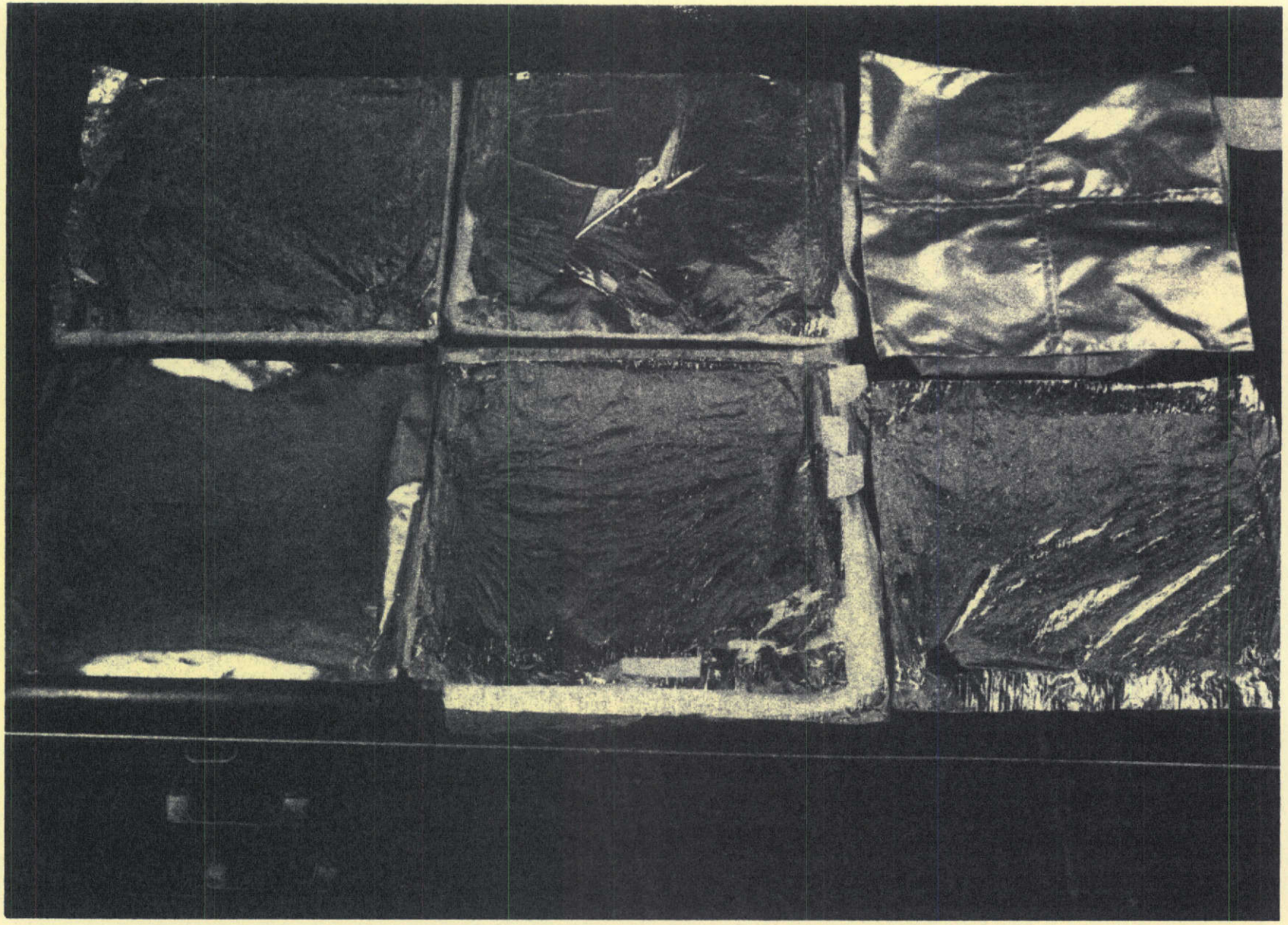

FIGURE 11 SAMPLES AFTER RUN – REMOVED FROM SETUP – FIRST DAY

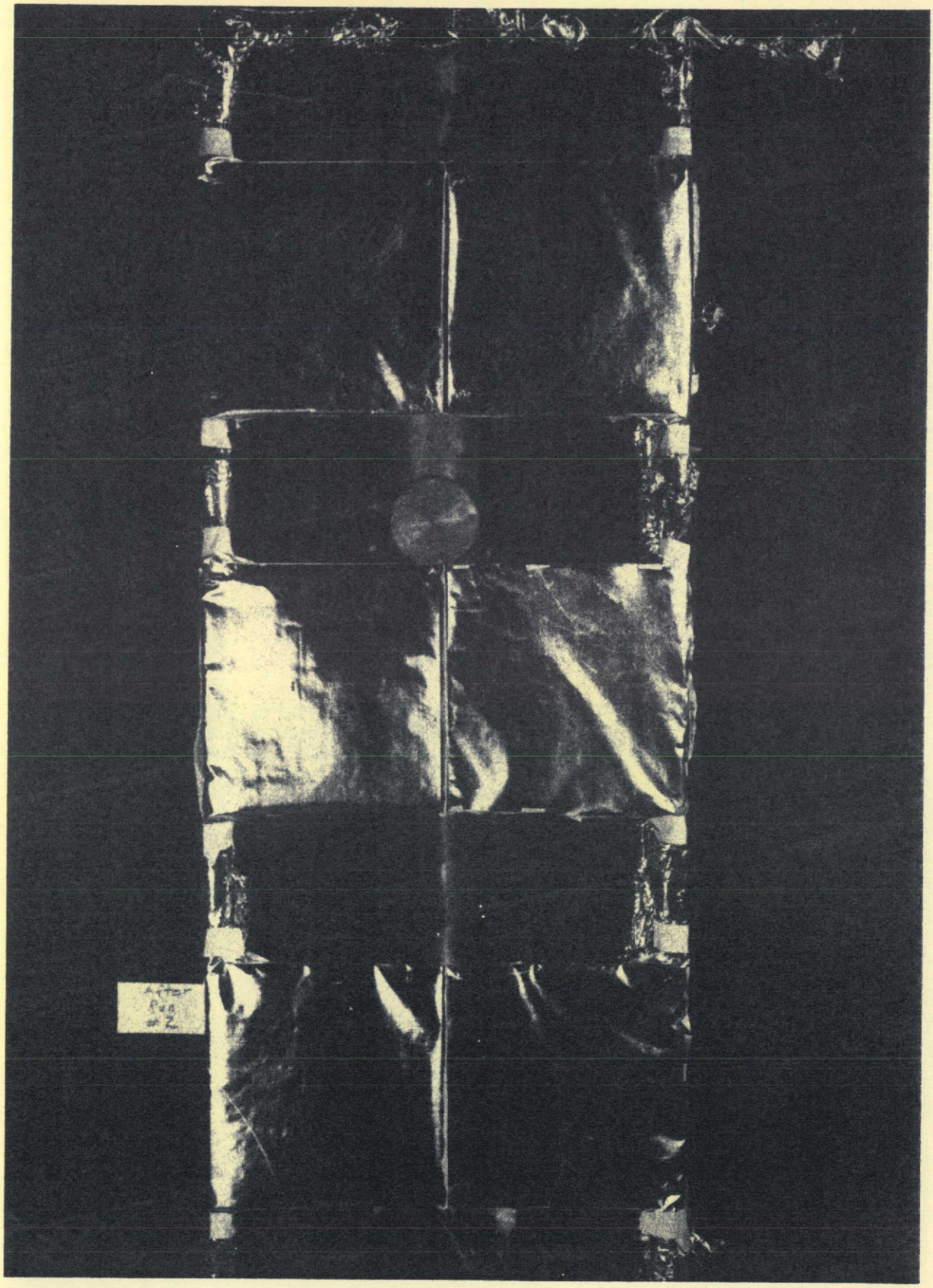

FIGURE 12 SAMPLES AFTER TEST – SECOND DAY

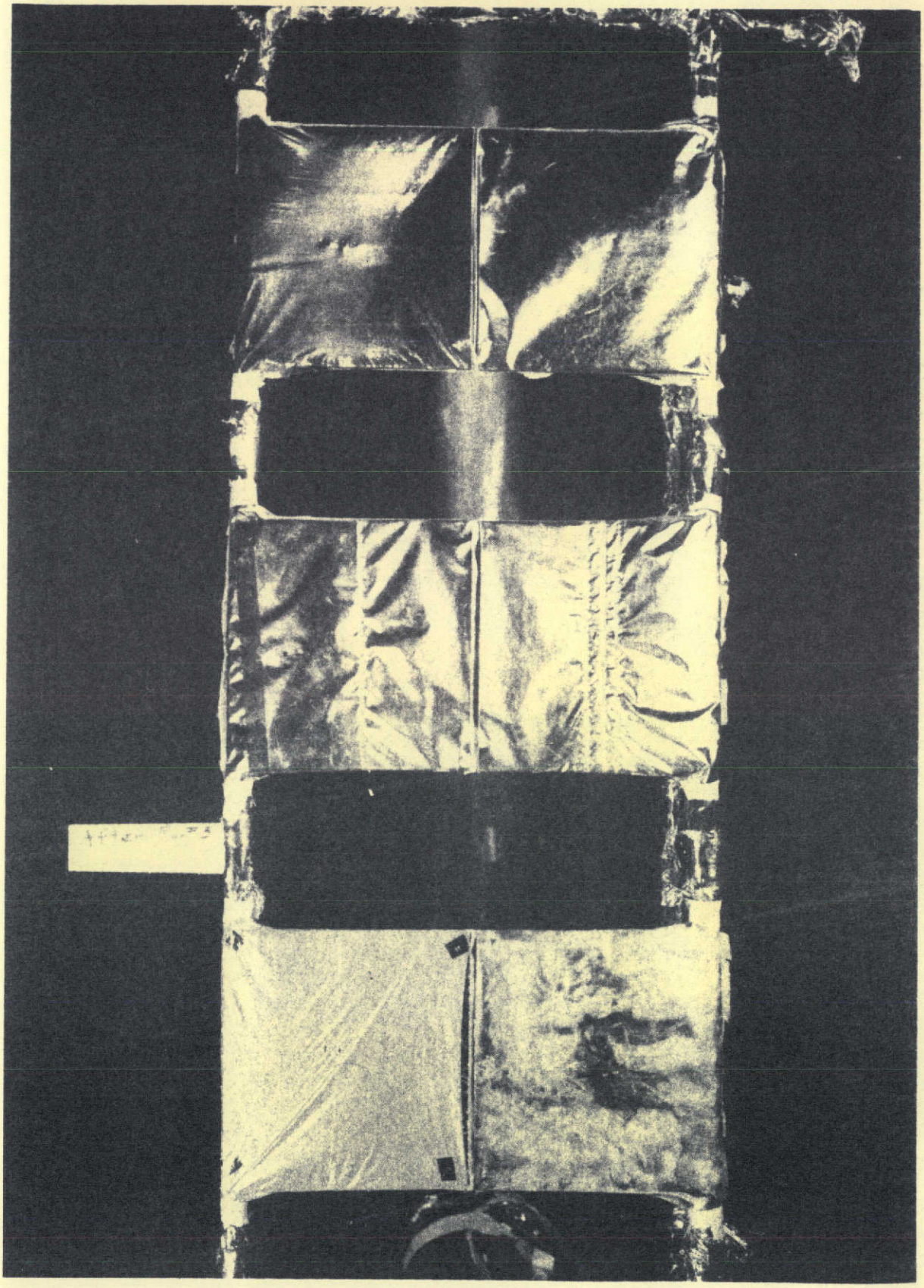

FIGURE 13 SAMPLES AFTER RUN – THIRD DAY

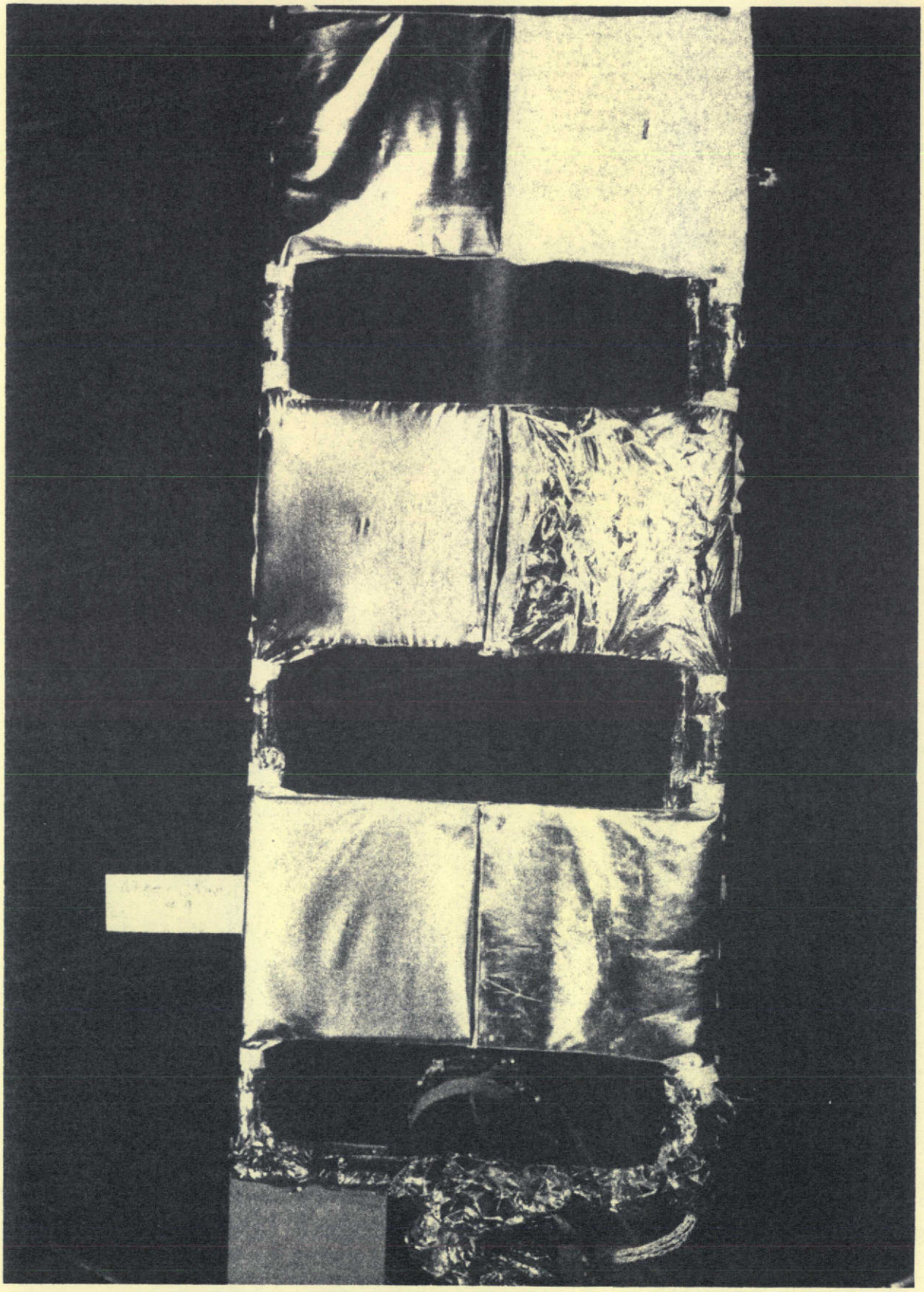

FIGURE 14 SAMPLES AFTER RUN – FOURTH DAY

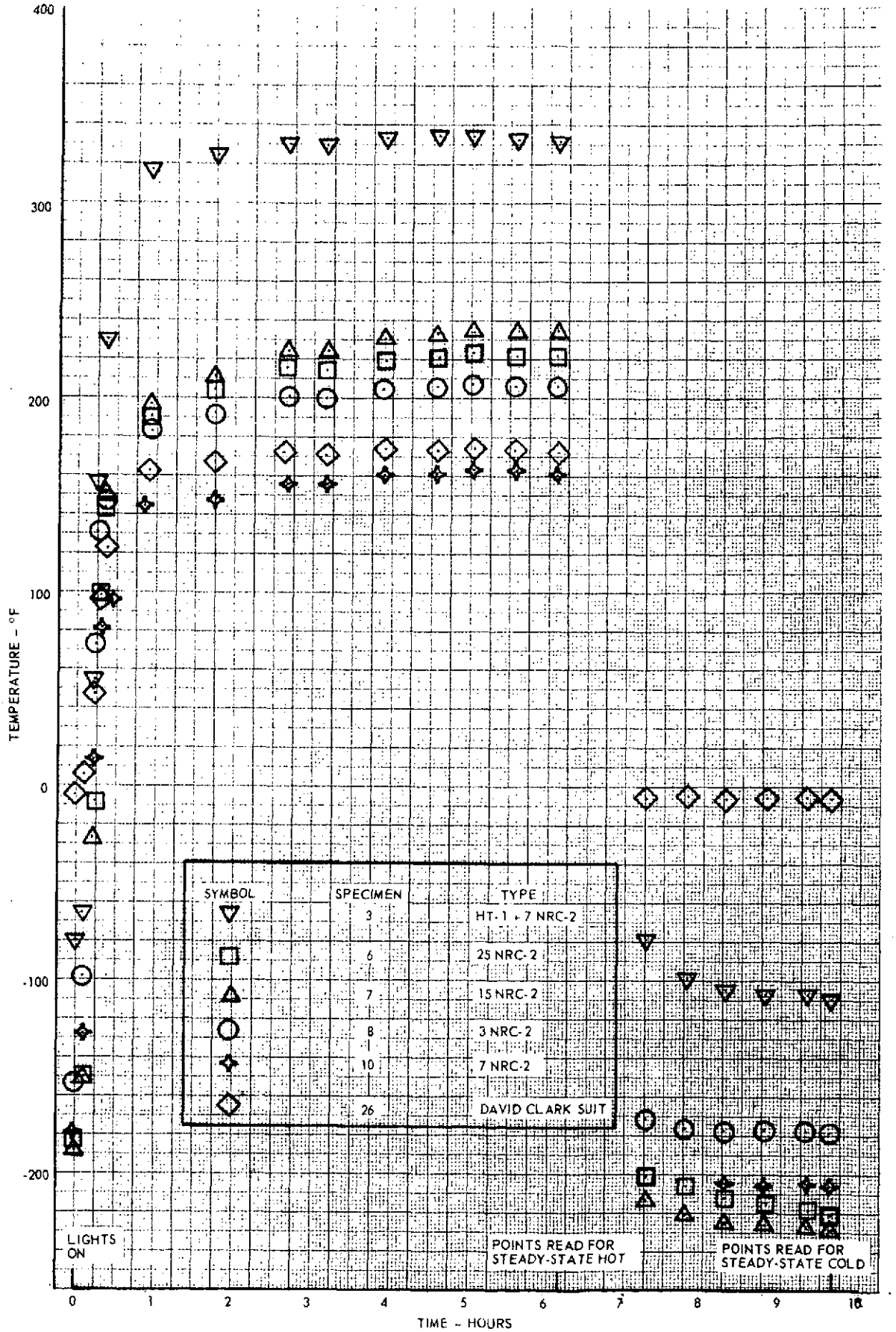

FIGURE 15 SURFACE TEMPERATURE VS TIME, TEST DAY NUMBER 1

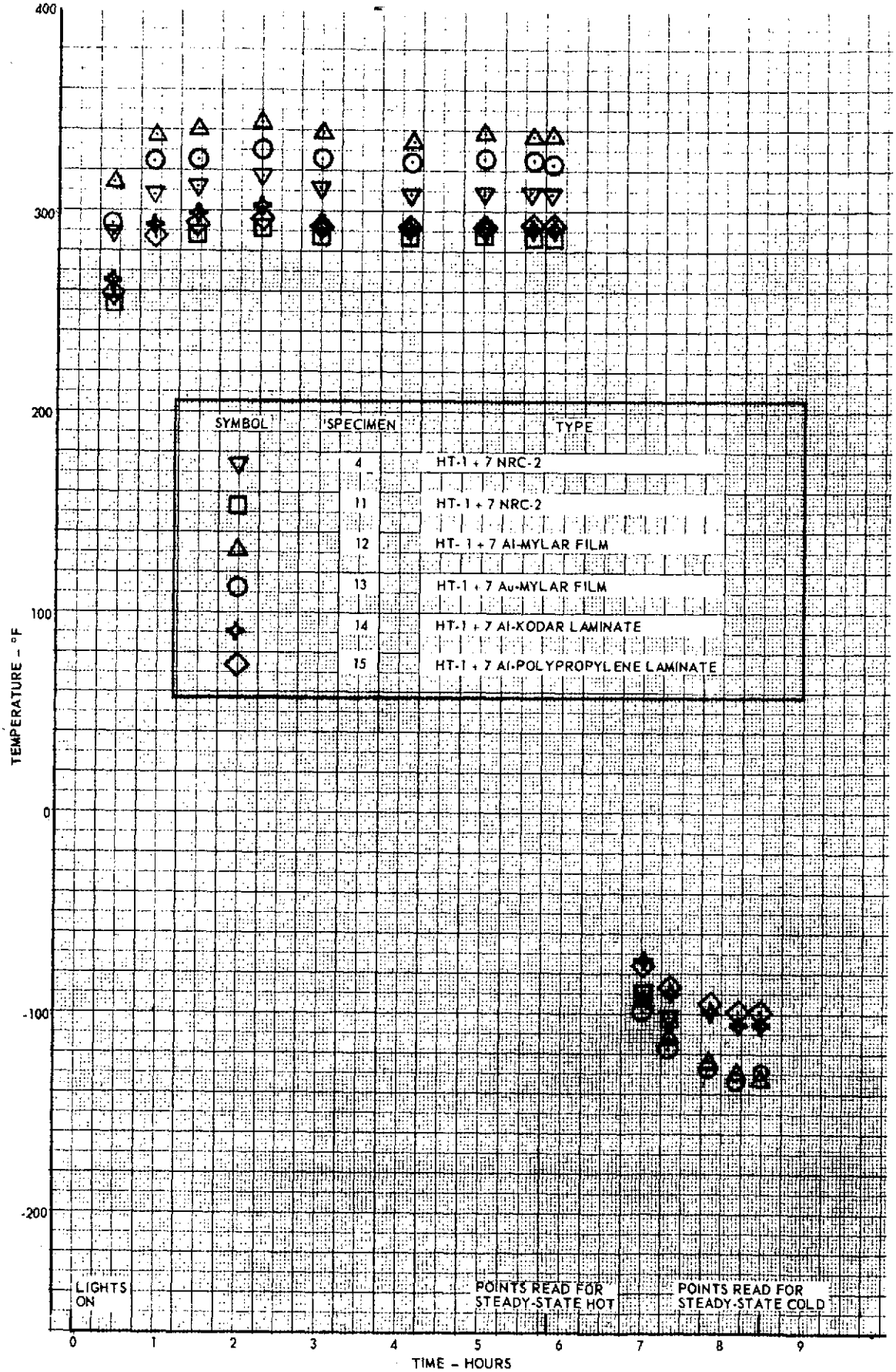

FIGURE 16 SURFACE TEMPERATURES VS TIME, TEST DAY NUMBER 2

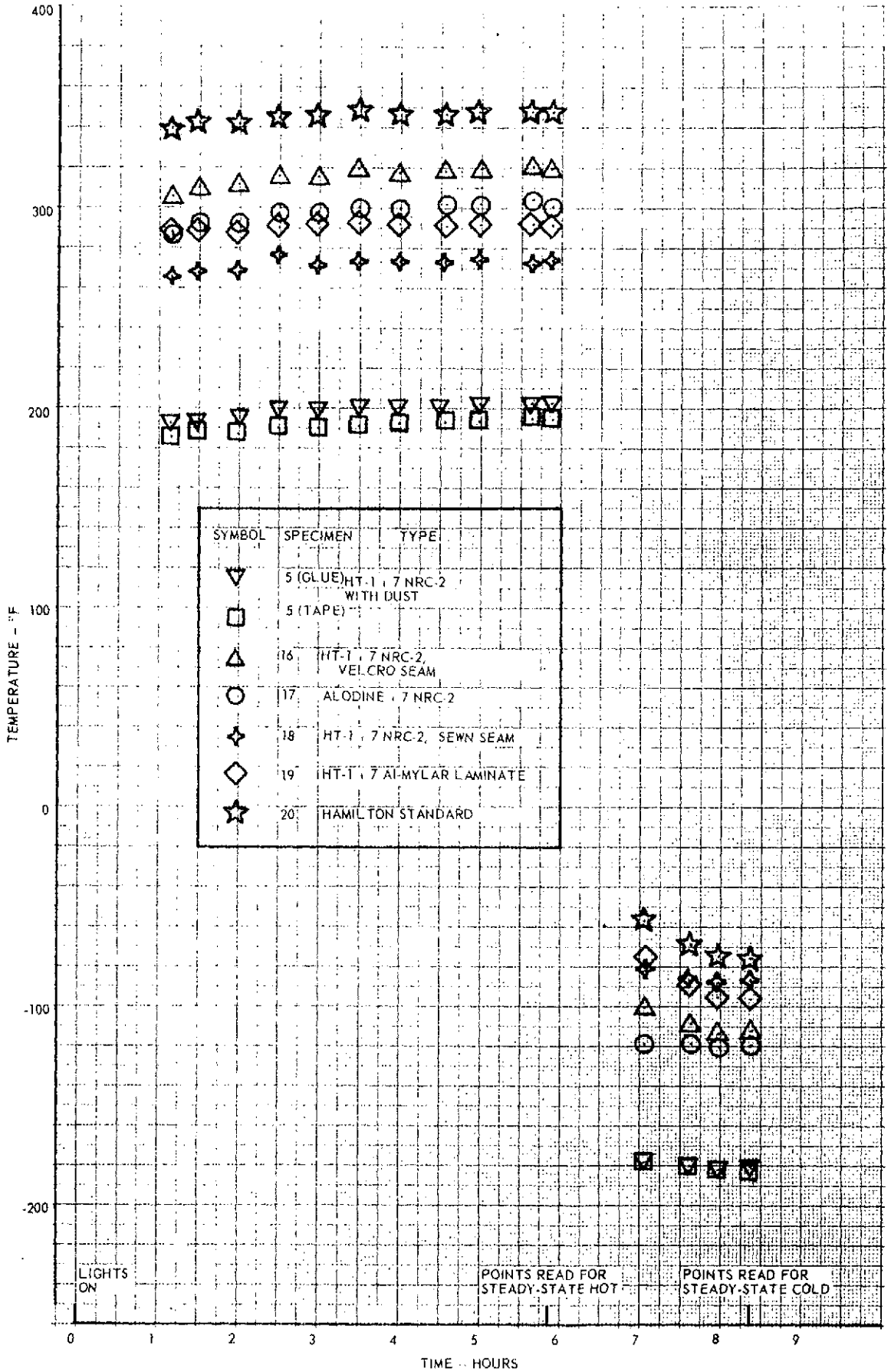

FIGURE 17 SURFACE TEMPERATURES VS TIME, TEST DAY NUMBER 3

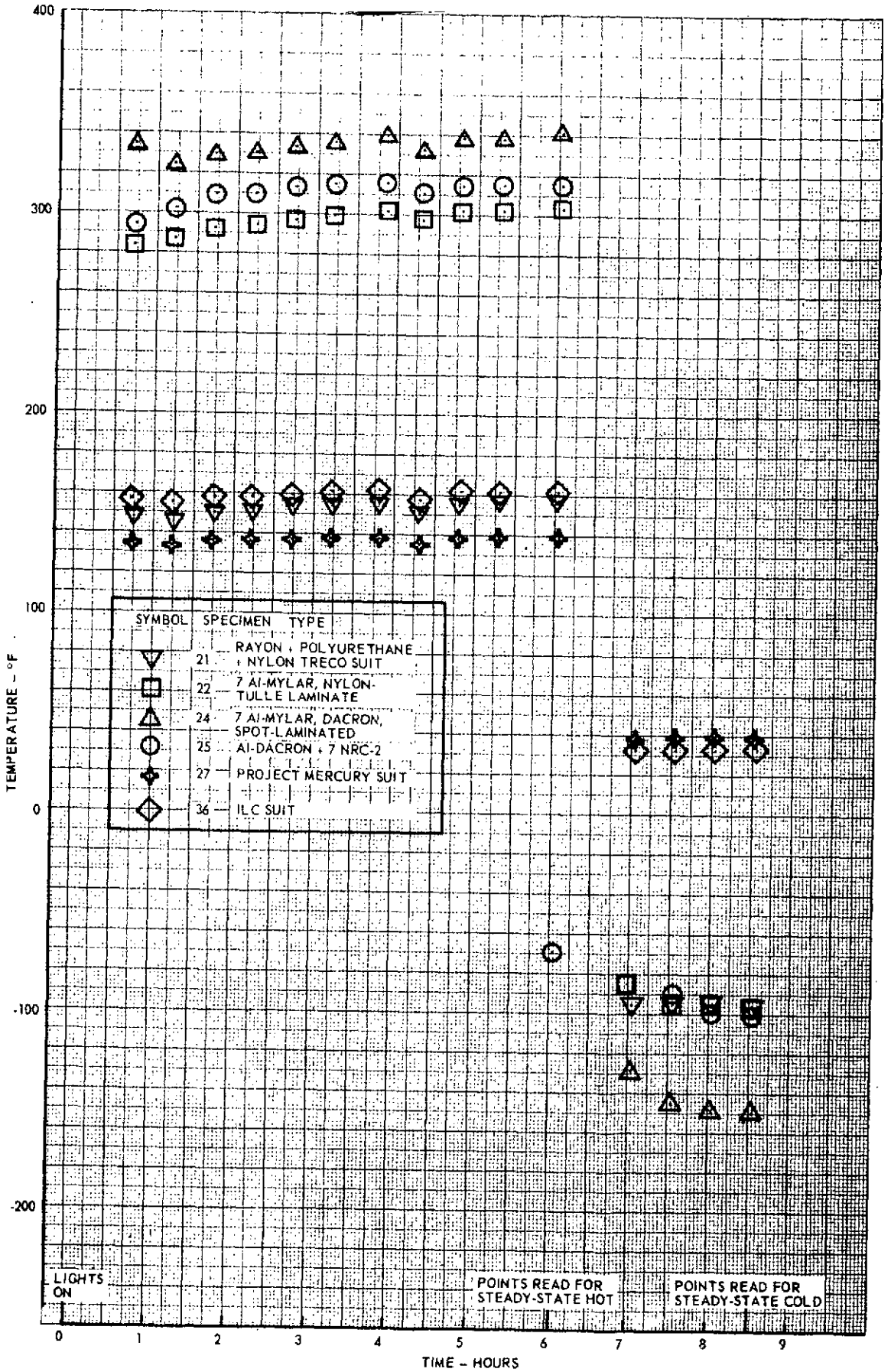

FIGURE 18 SURFACE TEMPERATURES VS TIME, TEST DAY NUMBER 4

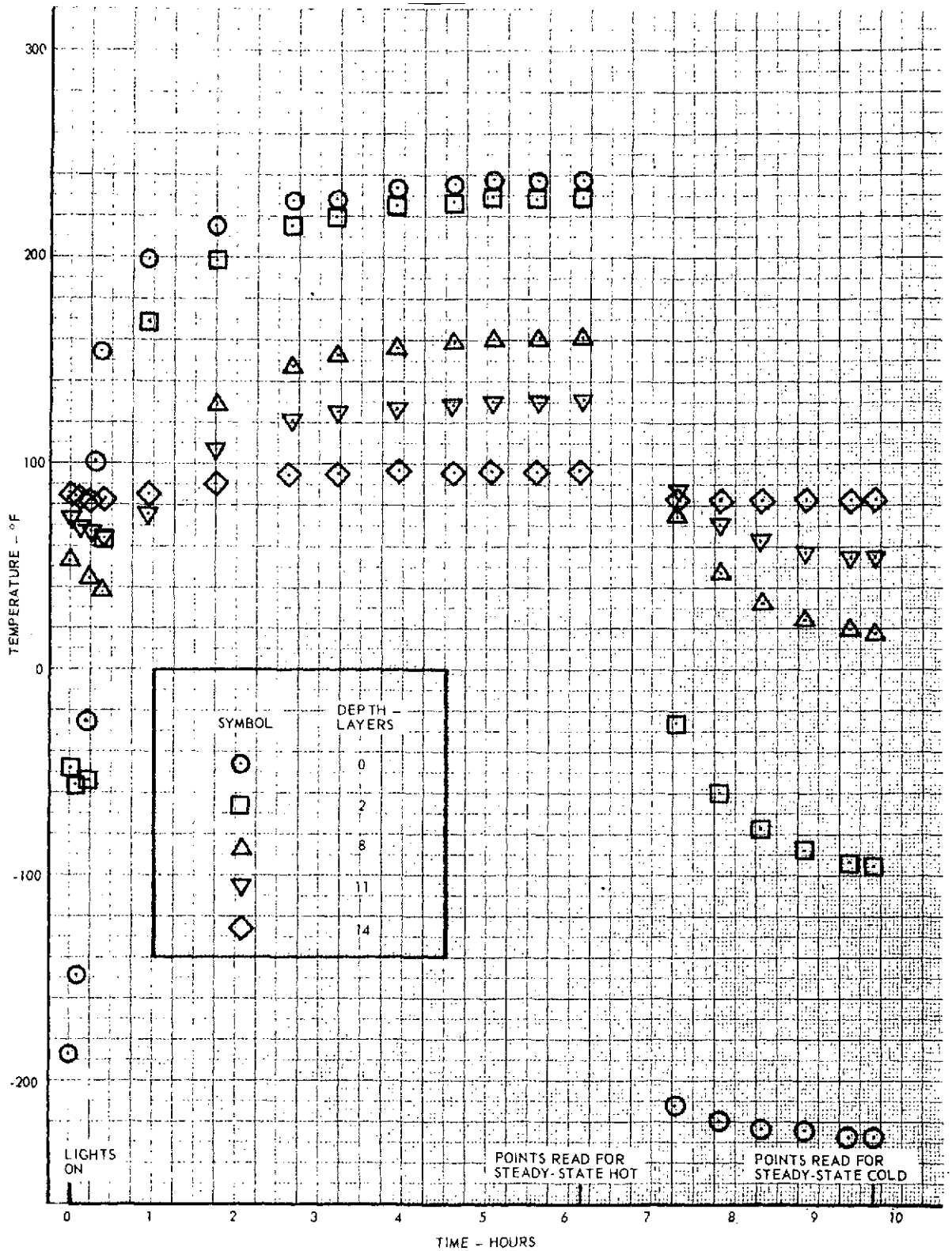

FIGURE 19 TEMPERATURE DISTRIBUTION VS TIME FOR SPECIMEN NUMBER 7 (NRC-2, 15 LAYERS)

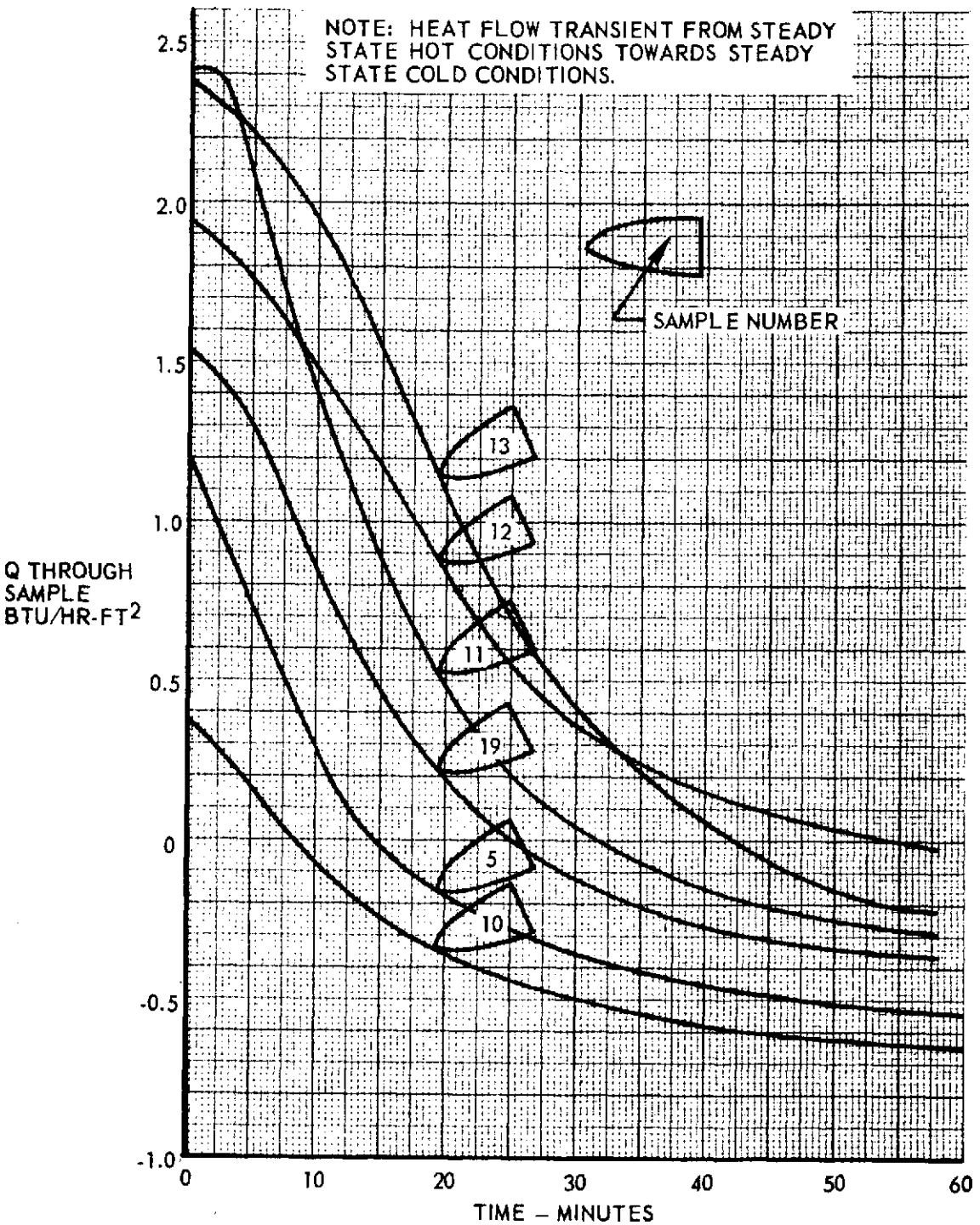

FIGURE 20 ENERGY FLOW TRANSIENTS – SAMPLES 5, 10, 11, 12, 13, 19

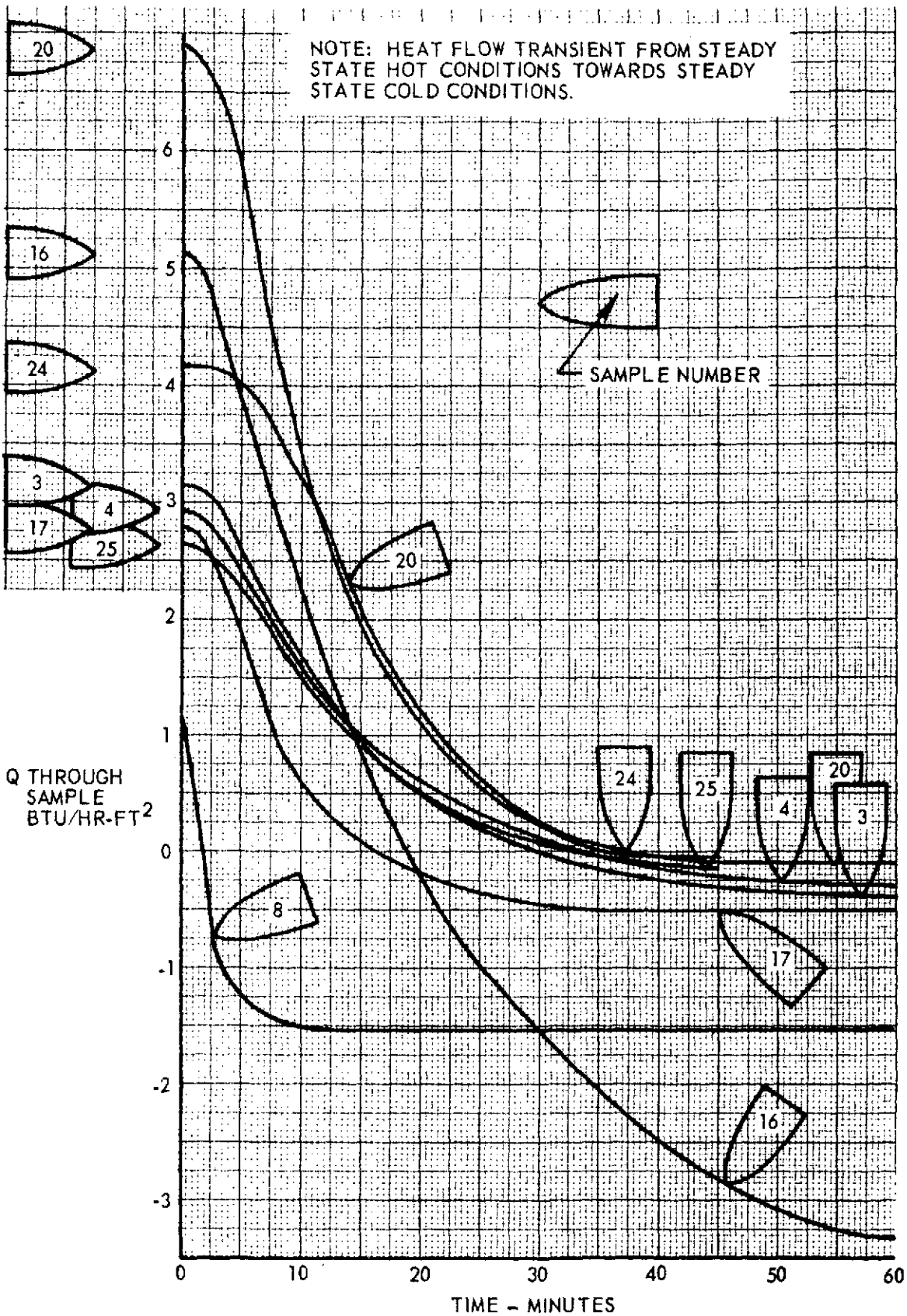

FIGURE 21 ENERGY FLOW TRANSIENTS - SAMPLES 3, 4, 16, 17, 20, 24, 25

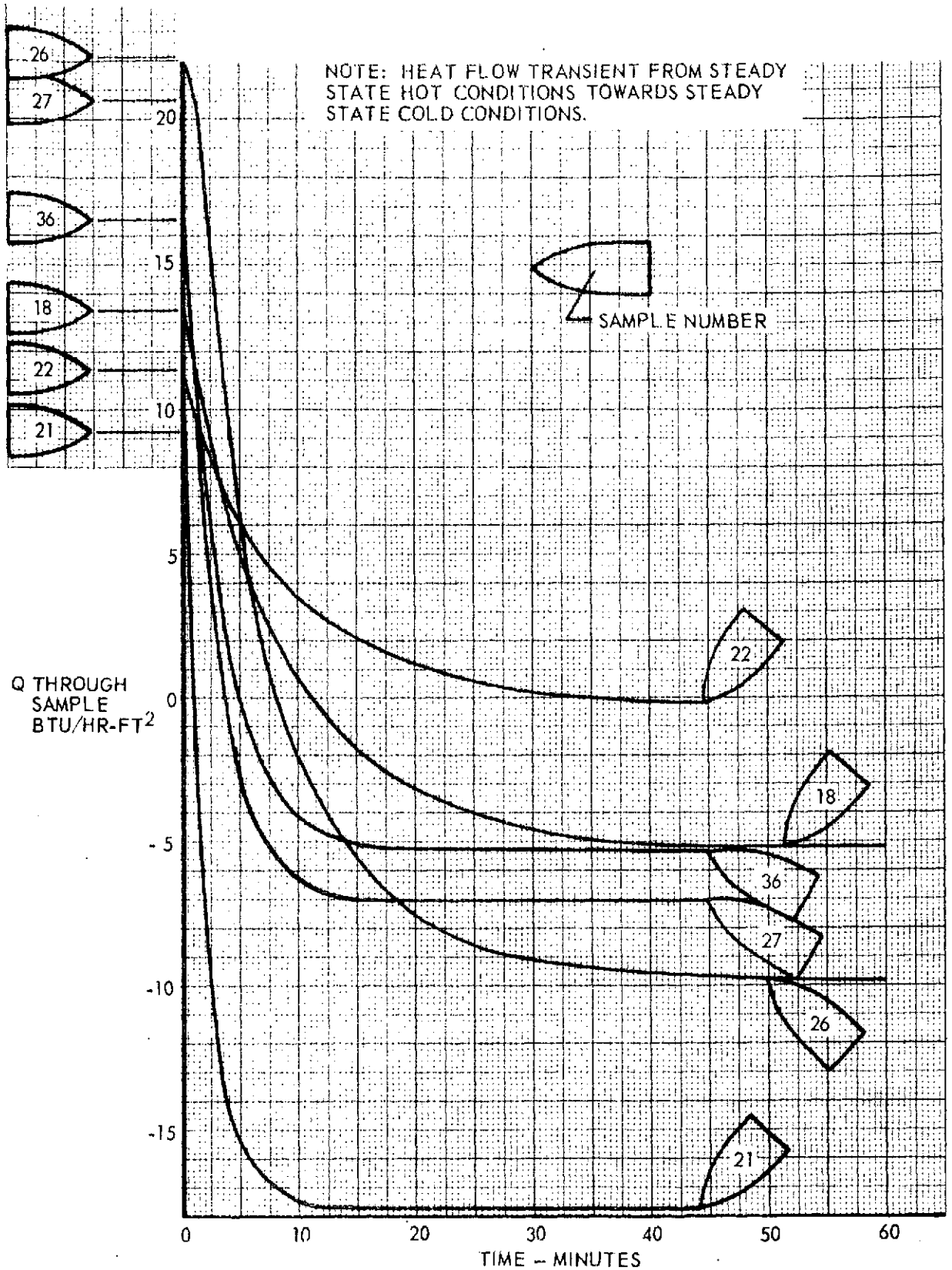

FIGURE 22 ENERGY FLOW TRANSIENTS – SAMPLES 18, 21, 22, 26, 27, 36

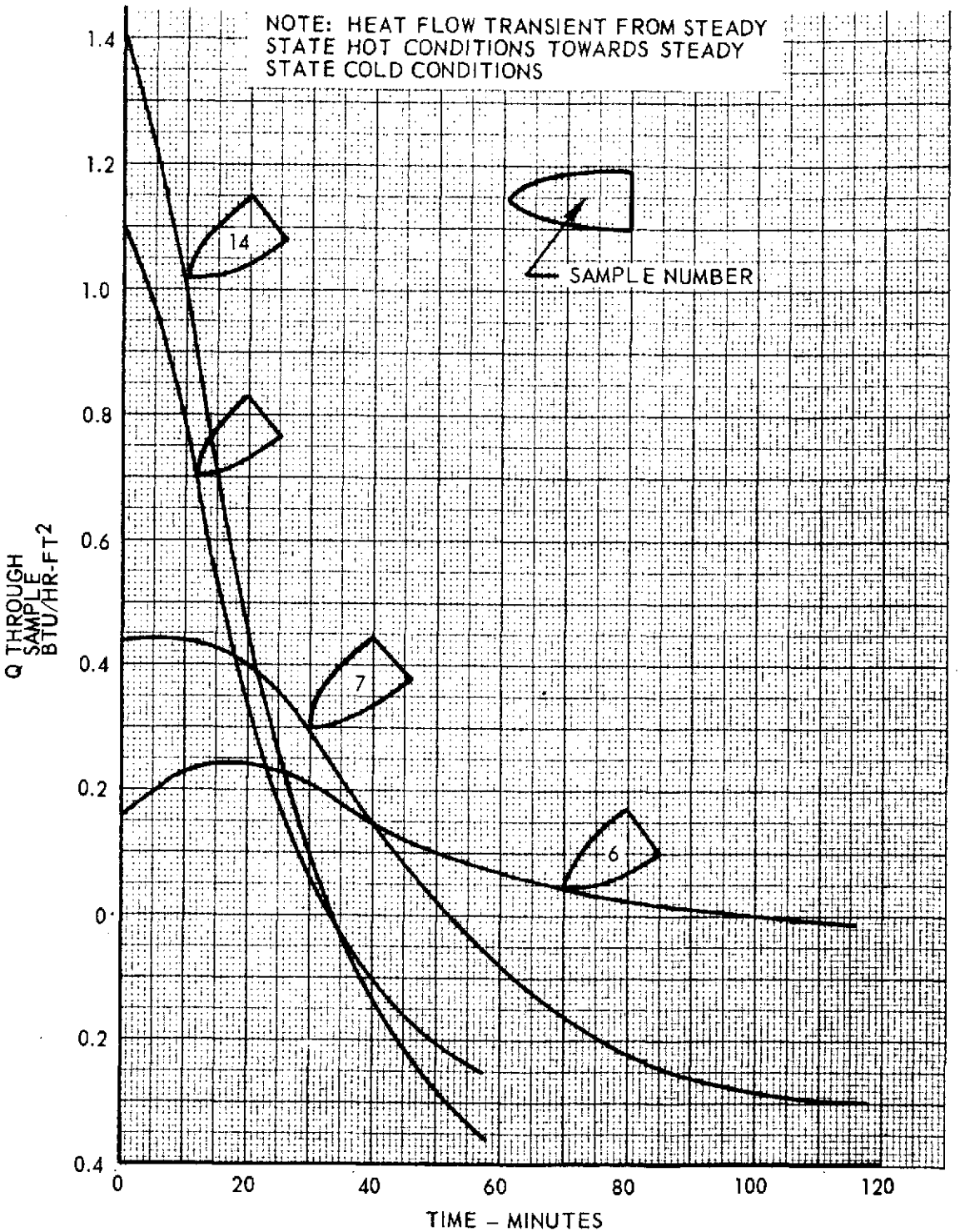

FIGURE 23 ENERGY FLOW TRANSIENTS – SAMPLES 6, 7, 14, 15

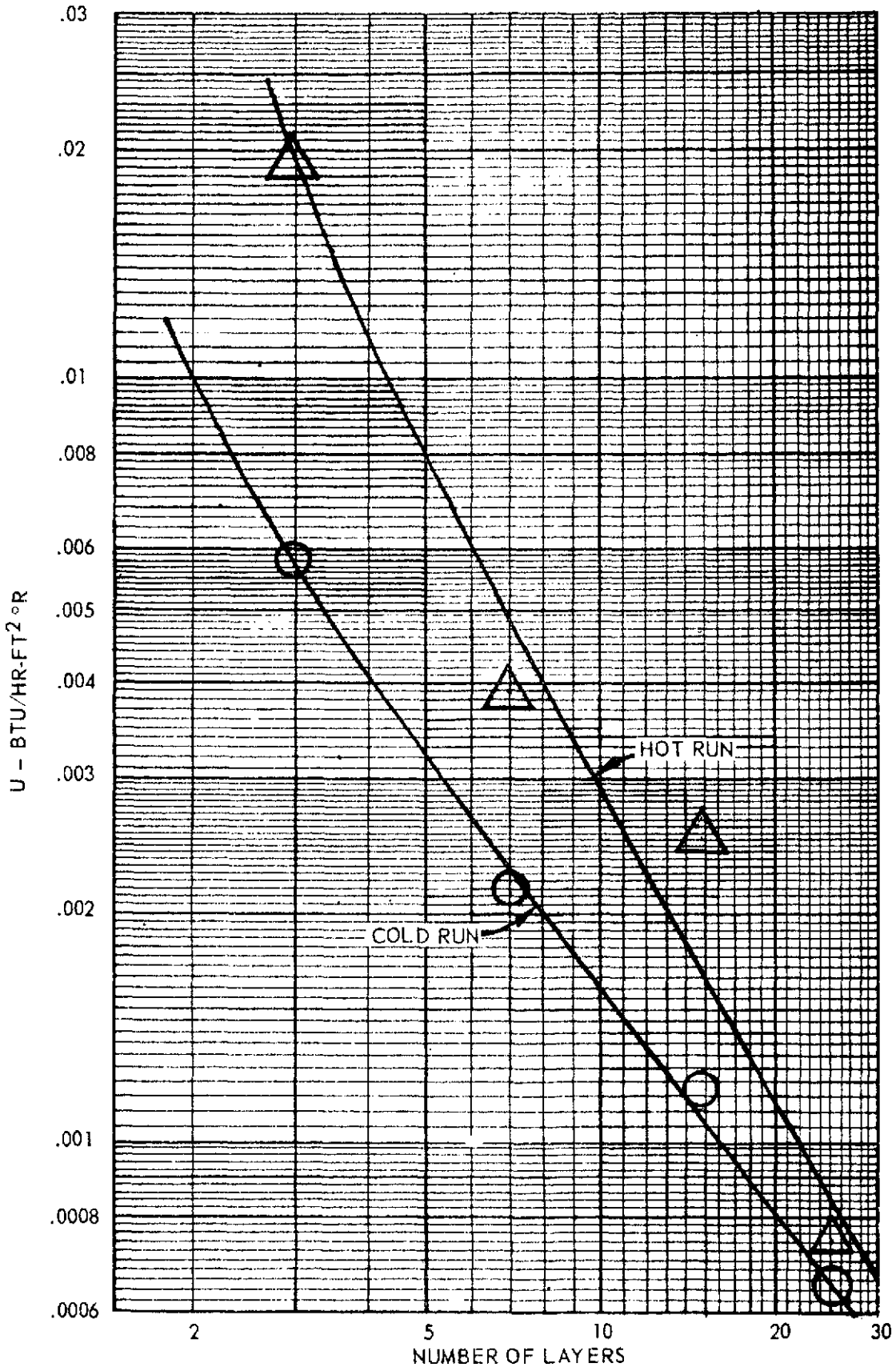

FIGURE 24 OVER-ALL COEFFICIENT OF HEAT TRANSFER VERSUS NRC-2 THICKNESS WITH DACRON SPACERS AND NO COVER

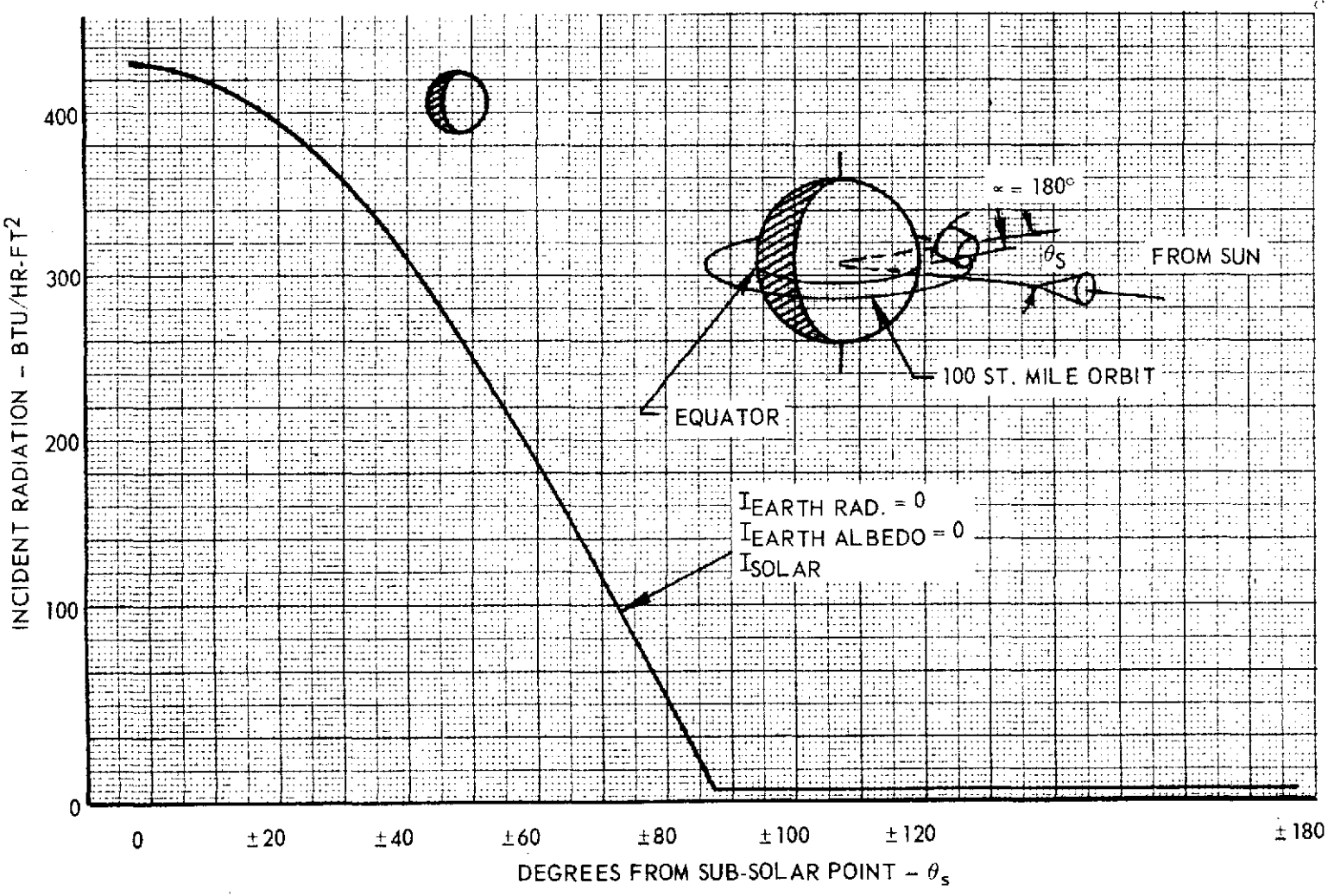

FIGURE 25 MAXIMUM LOCAL INCIDENT RADIATIONS VS ANGLE FROM SUB-SOLAR POINT, $\propto$ = 180°, FOR EARTH OR LUNAR ORBIT

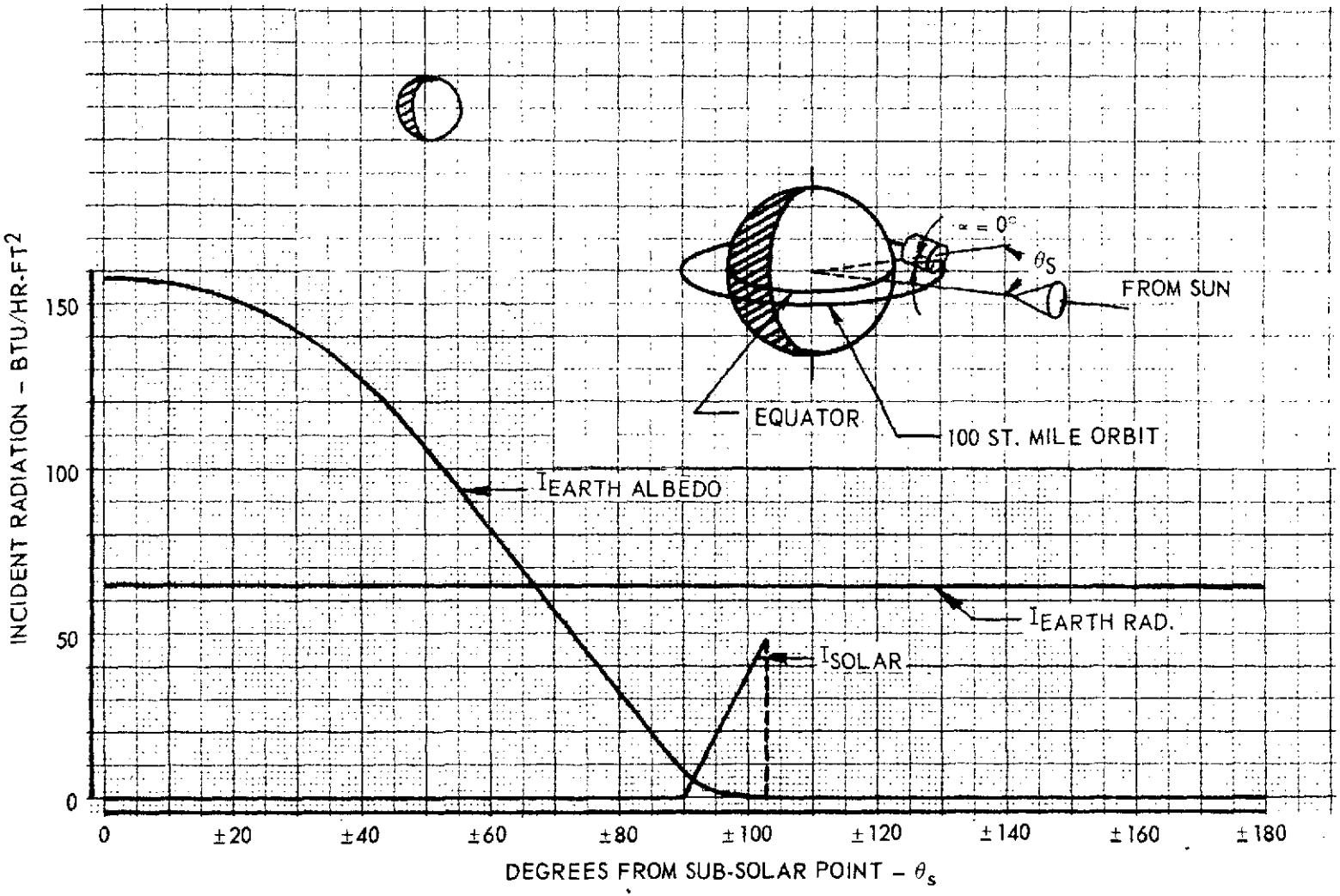

FIGURE 26 MAXIMUM LOCAL INCIDENT RADIATIONS VS ANGLE FROM SUB-SOLAR POINT, $\alpha = 0°$, FOR EARTH ORBIT

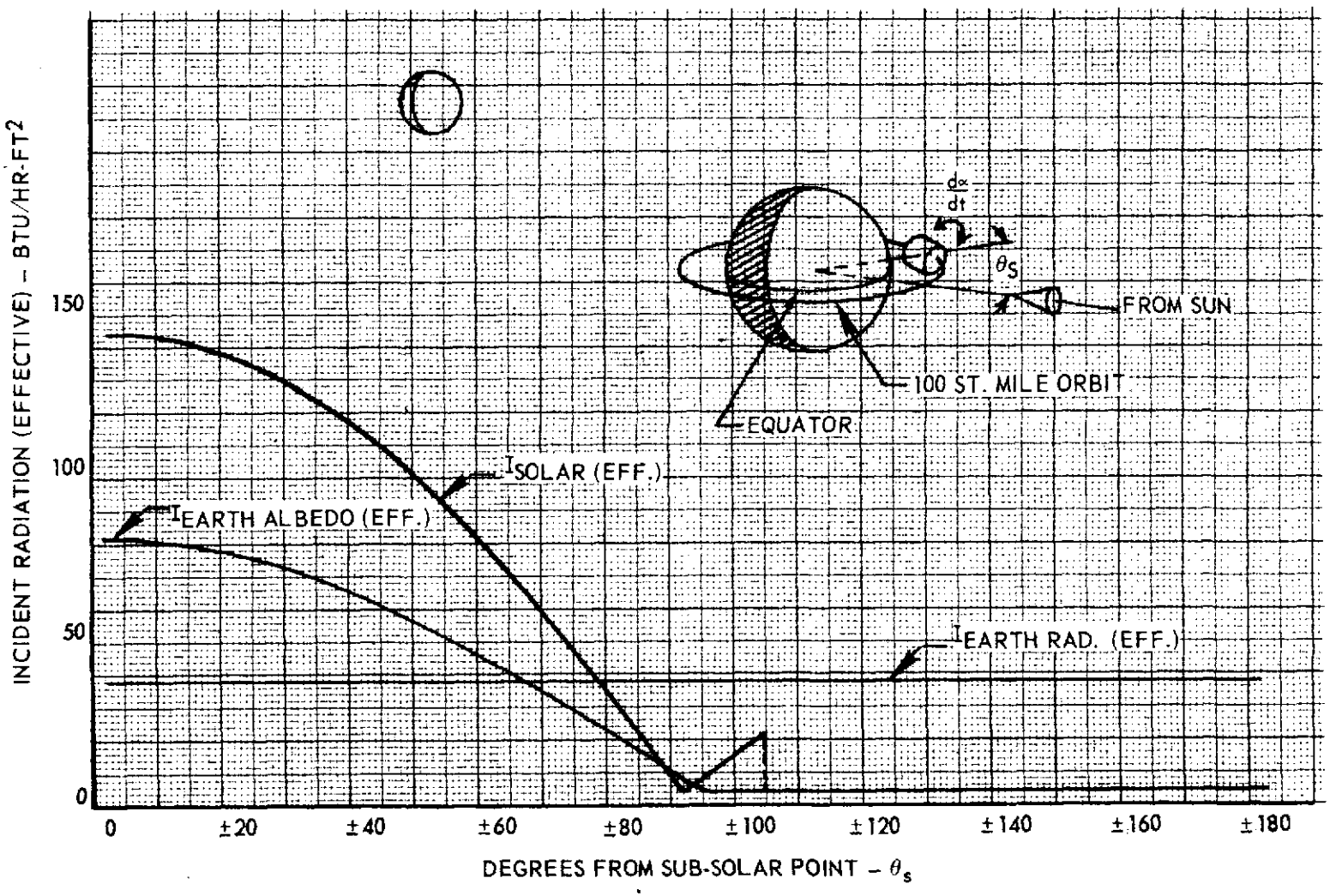

FIGURE 27 MAXIMUM TOTAL INCIDENT RADIATIONS VS ANGLE FROM SUB-SOLAR POINT, $d\alpha/dt > 0$, FOR EARTH ORBIT

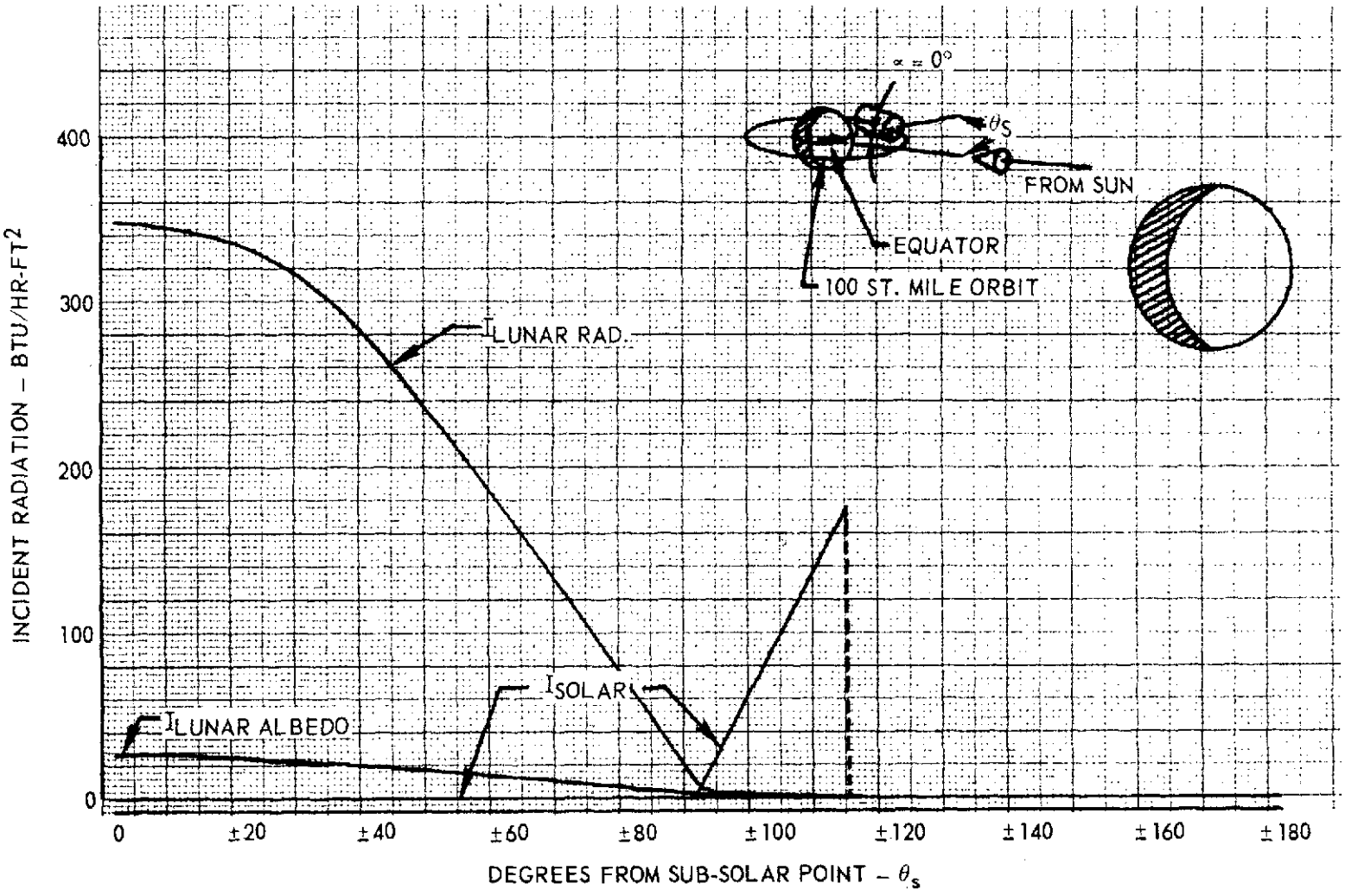

FIGURE 28 MAXIMUM LOCAL INCIDENT RADIATION VS ANGLE FROM SUB-SOLAR POINT, $\alpha = 0°$, FOR LUNAR ORBIT

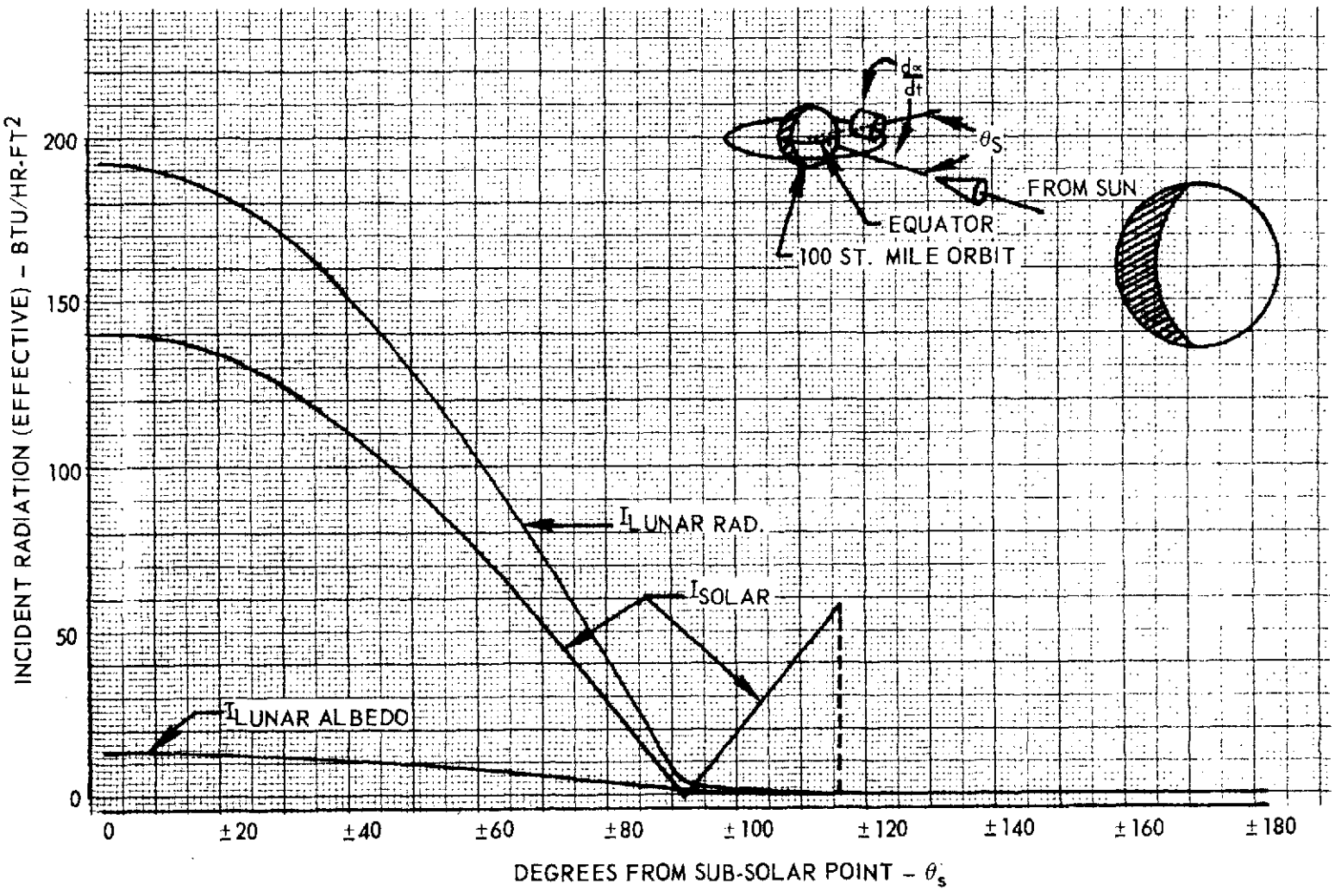

FIGURE 29 MAXIMUM TOTAL INCIDENT RADIATIONS VS ANGLE FROM SUB-SOLAR POINT, $d\alpha/dt > 0°$, FOR LUNAR ORBIT

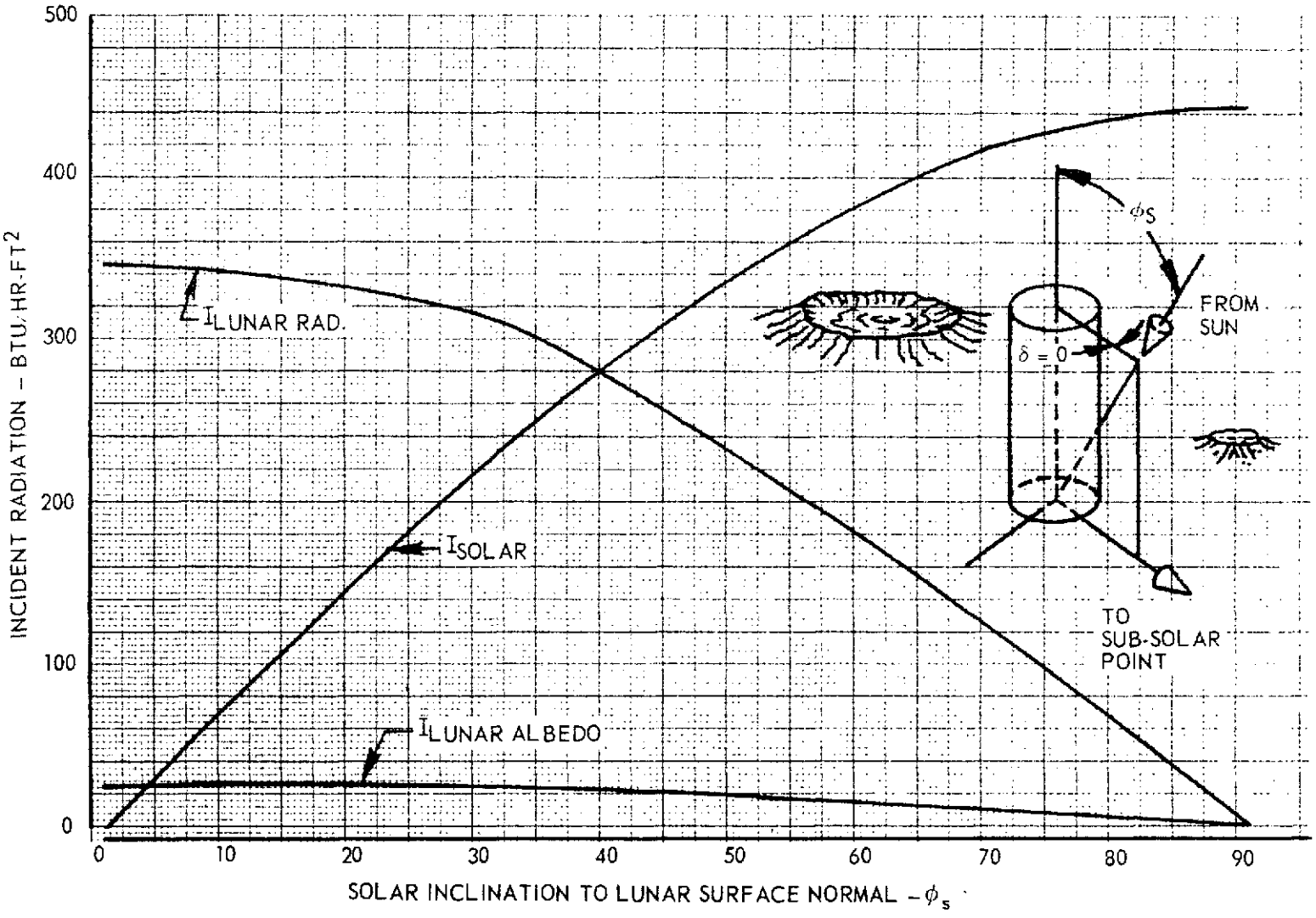

FIGURE 30 MAXIMUM LOCAL INCIDENT RADIATIONS VS SOLAR INCLINATION TO LUNAR SURFACE NORMAL AT $\delta = 0°$

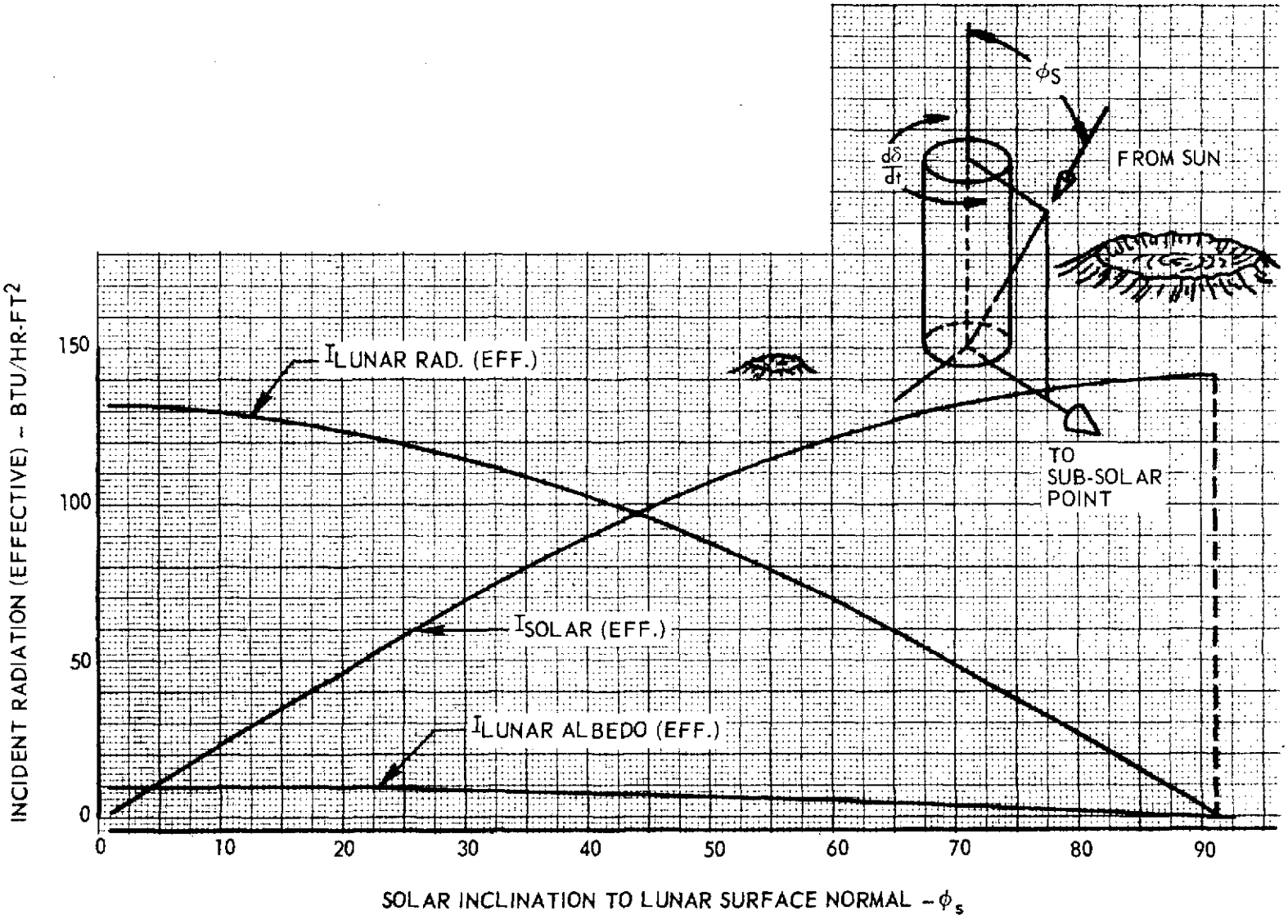

FIGURE 31 MAXIMUM TOTAL INCIDENT RADIATIONS VS SOLAR INCLINATION TO LUNAR SURFACE NORMAL AT $d\delta/dt > 0$

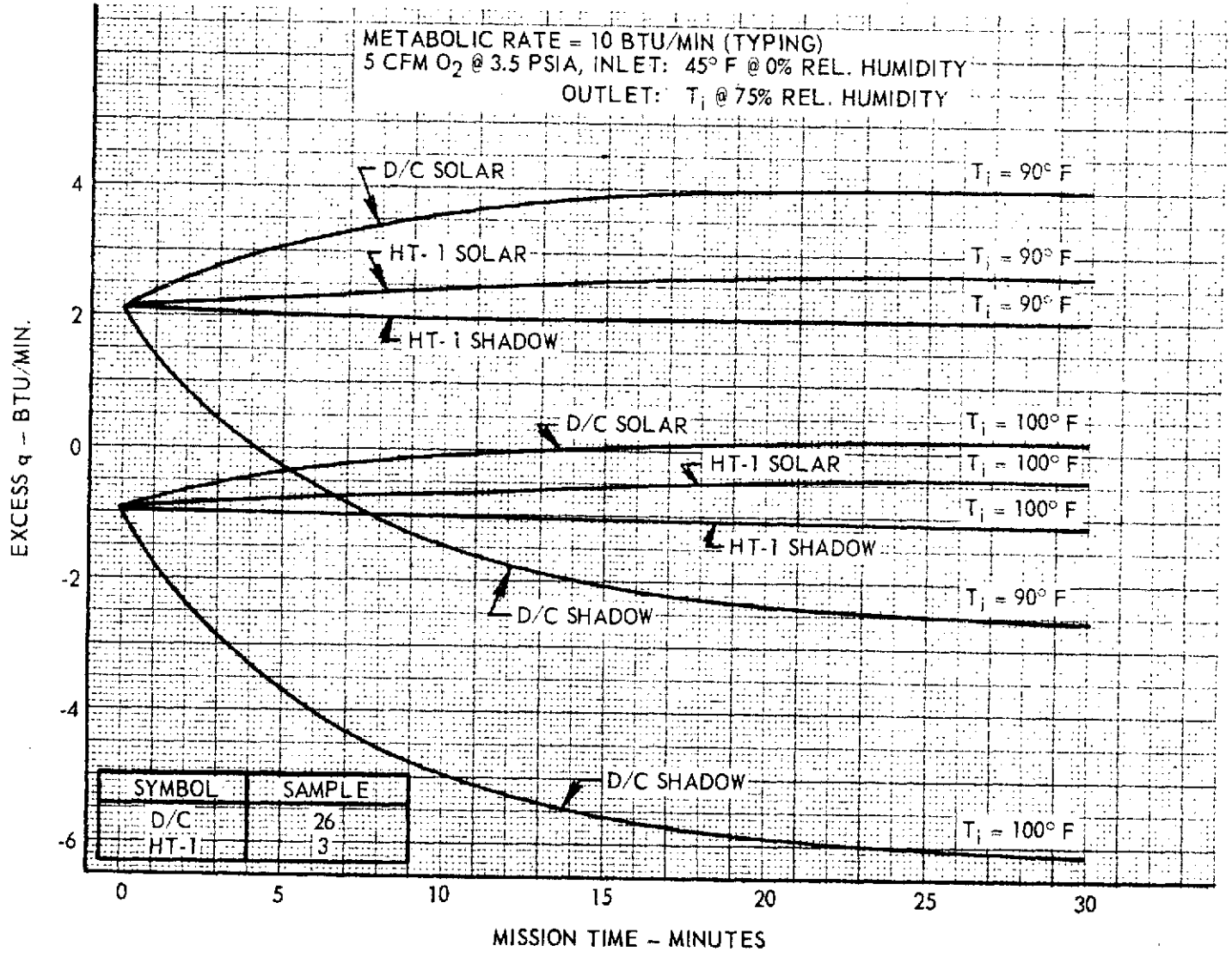

FIGURE 32 EXCESS HEATING RATE VS TIME FOR CONSTANT INNER WALL TEMPERATURES (T_i)

T A B L E S

TABLE 1

TEST SAMPLE MATERIALS

SAMPLE GROUP	SAMPLE NUMBER	NUMBER OF INNER LAYERS	COVER LAYER	INNER LAYER	SPACER LAYER	REMARKS
Optimum Layers	8	3	No separate cover	National Research Corp. NRC-2 insulation, 1/4 mil thick mylar with 0.001 mil aluminum on one side	Non-woven dacron 1 mil thick, 15 grams/yd.^{2}	Aluminum coating vacuum deposited on mylar. Mylar side turned to face simulated solar source
	10	7				
	7	15				
	6	25				
Other Multi Layers	12	7	DuPont HT-1 fabric with Minnesota Mining and Manufacturing aluminized coating on one side	1/4 mil mylar with vacuum deposited aluminum film on both sides		Supplier was G. T. Schjeldahl Company.
	13	7		1/4 mil mylar with vacuum deposited gold film on one side		Mylar side turned to face simulated solar source.
	14	7		0.45 mil Kodar laminated to 0.20 mil aluminum foil		Kodar side turned to face simulated solar source. Kodar made by Kodak Co. Sample supplier was Schjeldahl Company.
	15	7		0.45 mil polypropylene laminated to 0.18 mil aluminum foil		Polypropylene side turned to face simulated solar source. Sample supplied by Schjeldahl Company.
	19	7		1/3 mil laminated to 0.18 mil aluminum foil		Mylar faced simulated solar source. Supplier was Schjeldahl Company.
Pressure Suits	21	3	Rayon yarn dipped in Teflon containing a pigmentation of MgO	Two 1/8" layers of open celled polyurethane foam. One final layer of nylon Treco		Cover woven into 2 over 2 twill. Coarser rayon side faced simulated solar source. Supplier was B. F. Goodrich
	26	2	HT-1 fabric with cross seams	One layer-Teflon link net. Final layer-Nylon neoprene coated bladder cloth with cross seams.		Supplier was David Clark Co.
	27	1	Nylon fabric with aluminized surface	Transparent yellow colored plastic (Estane)		Project Mercury Suit. Supplier was B. F. Goodrich
	36	2		One layer-gray colored nylon final layer-black nylon with neoprene coated inside.		ILC Suit

TABLE 1

TEST SAMPLE MATERIALS

SAMPLE GROUP	SAMPLE NUMBER	NUMBER OF INNER LAYERS	COVER LAYER	INNER LAYER	SPACER LAYER	REMARKS
Environmental Effects	4	7	DuPont HT-1 fabric with MMM aluminized coating on one side	National Research Corp. NRC-2 insulation, 1/4 mil thick mylar with 0.001 mil aluminum on one side	Non-woven dacron, 1 mil thick 15 grams/yd.^{2}	Mylar side turned to face simulated solar source
	5	7	DuPont HT-1 fabric with MMM aluminized coating plus basaltic dust spread on aluminized surface.			Mylar side faced simulated solar source. Simulated moon dust furnished by Jet Propulsion Laboratories
Construction Techniques	3	7	Identical with Sample number 4			
	16	7	HT-1 fabric (two pieces) joined in middle with Velcro seam	Identical with Sample number 4		
	18	7	HT-1 fabric (two pieces) joined in middle with sewn seam (fold-back technique)	Identical with Sample number 4		
Other Samples	17	7	Mylar-Al laminate with alodine coating on aluminum side	NRC-2 insulation	Non-woven dacron	Aluminum side of cover and mylar side of inner layers faced simulated solar source, Supplier was Schjeldahl Co.
	20	7	Aluminized woven cover material	Aluminized mylar	Woven dacron scrim, 8 mil thick, 25.9 grams/yd.^{2}	Aluminum side of inner layers faced simulated solar source. Supplier was Hamilton Standard
	22	7	No separate cover	Aluminized mylar, 1/4 mil	Nylon tulle material	Inner layers laminated to spacer layers. Supplier was Schjeldahl Co.
	24	7	No separate cover	Aluminized Mylar, 1/4 mil	Dacron scrim	Inner layers spot laminated to each other. Supplier was Schjeldahl Co.
	25	7	Aluminized dacron, 0.01 inch thick, 7.75 ounces/yd.^{2}	NRC-2 insulation	Non-woven dacron	Cover supplied by Minnesota Mining and Manufacturing Co.
HT-1 Cover Samples	11	7	Identical with Sample number 4			
	3,4,5,11,12, 13,14,15,16 18,19	7	See detail descriptions in other sections of this table			

TABLE 2

SPECTRAL ENERGY DISTRIBUTION, SES

Wavelength λ(mμ)	Energy mw cm^{-2}	Wavelength λ(mμ)	Energy mw cm^{-2}
260	(0.5)	560-70	0.2
260-70	1.0	70-80	2.7
70-80	1.5	80-90	2.2
80-90	1.7	590-600	0.2
290-300	2.0	600-10	1.0
300-10	2.5	10-20	0.6
10-20	2.6	20-30	0.1
20-30	0.4	30-40	0.1
30-40	1.2	40-50	0.1
40-50	0.2	50-60	0.1
50-60	0.4	60-70	0.1
60-70	3.6	70-80	1.1
70-80	0.5	80-90	0.4
80-90	0.3	690-700	0.1
390-400	0.2	700-750	0.5
400-10	1.7	750-800	0.4
10-20	0.2	800-850	0.7
20-30	0.3	850-900	1.0
30-40	3.4	900-950	0.9
40-50	0.2	950-1000	1.0
50-60	0.2	1000-1100	2.0
60-70	0.1	1100-1200	1.8
70-80	0.1	1200-1300	0.9
80-90	0.1	1300-1400	1.9
490-500	0.2	1400-1500	0.4
500-10	0.1	1500-1600	0.5
10-20	0.1	1600-1700	0.5
20-30	0.1	1700-1800	0.5
30-40	0.2	1800-1900	0.2
40-50	2.5	1900-2000	0.1
550-60			

TABLE 3

TYPICAL HEAT FLUX DISTRIBUTION FOR A TEST POSITION

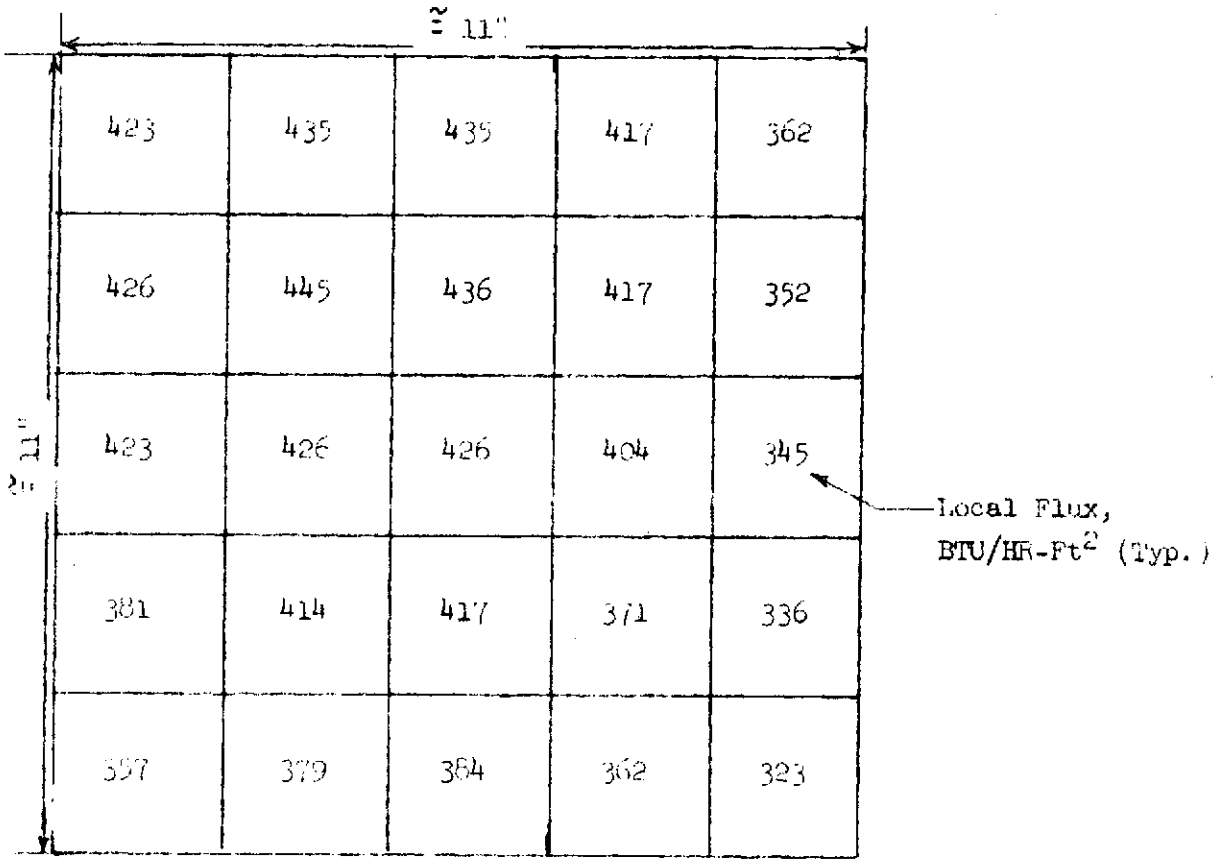

Pickup Centered at Position: 1 (Ref. Figure 2)

Date: 29 March 1963

Time: 12:00

Mean Flux Intensity for Entire Area: 396 $\frac{\text{BTU}}{\text{HR-Ft}^2}$

TABLE 4

TEST RESULTS, FIRST DAY

DATE: 5 APRIL 1963

SAMPLE NUMBER	SAMPLE DESCRIPTION	WEIGHT BEFORE / WEIGHT AFTER GRAMS	WEIGHT LOSS %	TEST POSITION	HEAT ± 5% $FLUX_{ses}$ BTU/HR-Ft^2	SURFACE TEMP. °F	BACK PLATE TEMP. °F	ΔT SURFACE BACK PLATE °F	Q HEAT FLOW BTU/HR-Ft^2	ϵ TEST	α/ϵ TEST	U BTU/HR-Ft^2-°R
3	HT-1 Cover + 7 layers NRC-2 (Control)			Lower Right (#6)	399	334	90	244	3.25		1.844- 2.236 2.04(avg)	.0133
3	HT-1 Cover + 7 layers NRC-2 (Control)	30.10 / 29.70	1.33	Lower Right	-	-108	90	198	-.54	.0208	-	.00273
6	25 layers NRC-2			Middle Left (#3)	486	224	89.5	134.5	.10		.747- .824 .785(avg)	.000743
6	25 layers NRC-2	68.31 / 68.20	0.18	Middle Left	-	-219	88.5	307.5	-.20	.0412	-	.00065
7	15 layers NRC-2			Middle Right (#4)	440	238	90	148	.37		.898- .991 .944(avg)	.0025
7	15 layers NRC-2	43.03 / 42.80	0.54	Middle Right	-	-227	89	316	-.37	.0796	-	.00117
8	3 layers NRC-2			Top Right (#2)	439	209	89.5	119.5	2.325		.783- .866 .824 (avg)	.01946
8	3 layers NRC-2	6.80 / 6.50	4.42	Top Right	-	-177	88.5	265.5	-1.54	.1482	-	.0058
10	7 layers NRC-2			Lower Left (#5)	383	164	89	75	.29		.659- .731 .695(avg)	.00387
10	7 layers NRC-2	18.95 / 18.80	0.79	Lower Left	-	-206	88.5	294.5	-.63	.1015	-	.00214
26	David Clark Suit			Top Left (#1)	411	175	91	84	26.9		.697- .771 .734(avg)	.32
26	David Clark Suit	163.53 / 163.53	0.00	Top Left	-	-5	90	95	-9.83	.1347	-	.1036

TABLE 5

TEST RESULTS, SECOND DAY

DATE: 9 APRIL 1963

SAMPLE NUMBER	SAMPLE DESCRIPTION	WEIGHT BEFORE / WEIGHT AFTER GRAMS	WEIGHT LOSS %	TEST POSITION	HEAT ± 5% $FLUX_{ses}$ BTU/HR-Ft^2	SURFACE TEMP. °F	BACK PLATE TEMP. °F	ΔT SURFACE BACK PLATE °F	Q HEAT FLOW BTU/HR-Ft^2	ϵ TEST	α/ϵ TEST	U BTU/HR-Ft^2-°R
4	HT-1 Cover + 7 layers NRC-2 (Control)			Lower Right (#6)	404	310	95	215	3.10		2.140-2.360 2.25(avg)	.0144
4	HT-1 Cover + 7 layers NRC-2 (Control)	29.13 / 28.37	2.62	Lower Right	-	-106	96	202	-.27	.01031	-	.001338
11	HT-1 Cover + 7 layers NRC-2 (Control)			Lower Left (#5)	385	289	93	196	2.52		1.788-1.972 1.88(avg)	.01285
11	HT-1 Cover + 7 layers NRC-2 (Control)	30.03 / 29.60	1.43	Lower Left	-	-107	94.7	201.7	-.363	.01404	-	.0018
12	HT-1 Cover + 7 layers Aluminum (both sides)			Middle Left (#3)	486	340	94	246	2.01		2.218-2.444 2.331(avg)	.00817
12	HT-1 Cover + 7 layers Aluminum (both sides)	29.00 / 28.60	1.42	Middle Left	-	-131	95	226	-.091	.00472	-	.000402
13	HT-1 Cover + 7 layers Gold (one side)-Mylar, Mylar up			Middle Right (#4)	443	327	94	233	2.47		1.793-1.988 1.89(avg)	.0106
13	HT-1 Cover + 7 layers gold (one side)-Mylar, Mylar up	28.09 / 27.70	1.39	Middle Right	-	-130	95	225	-.254	.01434	-	.001128
14	HT-1 Cover + 7 layers Kodar-Al laminate, Kodar up			Top Right (#2)	436	294	94	200	1.49		1.443-2.059 1.751(avg)	.00745
14	HT-1 Cover + 7 layers Kodar-Al laminate, Kodar up	48.655 / 48.15	1.04	Top Right	-	-103	95	198	-.395	.01458	-	.001995
15	HT-1 Cover + 7 layers Polypropylene-Al laminate			Top Left (#1)	412	295	95	200	1.20		1.556-1.725 1.64(avg)	.006
15	HT-1 Cover + 7 layers Polypropylene-Al laminate	40.29 / 40.1	0.47	Top Left	-	-100	96	196	-.296	.01053	-	.00151

69-a

69

TABLE 6

TEST RESULTS, THIRD DAY

DATE: 11 APRIL 1963

SAMPLE NUMBER	SAMPLE DESCRIPTION	WEIGHT BEFORE / WEIGHT AFTER GRAMS	WEIGHT LOSS %	TEST POSITION	HEAT ± 5% FLUX$_{ses}$ BTU/HR-Ft^2	SURFACE TEMP. °F	BACK PLATE TEMP. °F	△ T SURFACE BACK PLATE °F	Q HEAT FLOW BTU/HR-Ft^2	ϵ TEST	α/ϵ TEST	U BTU/HR-Ft^2-°R
5	HT-1 Cover + 7 layers NRC-2. Lunar dust on cover (hand oil)			Lower Right (#6)	407	203	92.5	110	.64		.808-.892 .850(avg)	.00582
5	HT-1 Cover + 7 layers NRC-2. Lunar dust on cover (hand oil)	29.4 / 29.2	0.68	Lower Right	-	-182	91	273	-.514	.0534	-	.00188
16	HT-1 Cover + 7 layers NRC-2 with Velcro Seam			Middle Left (#3)	490	321	92	229	5.2		NA	.0227
16	HT-1 Cover + 7 layers NRC-2 with Velcro Seam	43.1 / 42.1	2.32	Middle Left	-	-112	90	202	-3.30	NA	-	.01632
17	Al-Mylar Cover with Alodine coating on outside + 7 layers NRC-2			Lower Left (#5)	388	302	91.3	211	2.56		1.875-1.70 1.787(avg)	.0121
17	Al-Mylar Cover with Alodine coating on outside + 7 layers NRC-2	20.5 / 20.28	1.07	Lower Left	-	-119	90	209	-.521	.0232	-	.00249
18	HT-1 Cover + 7 layers NRC-2 with Sewn Seam (fold-back technique)			Middle Right (#4)	446	275	92	183	13.65		NA	.0746
18	HT-1 Cover + 7 layers NRC-2 with Sewn Seam (fold-back technique)	34.1 / 33.3	2.05	Middle Right	-	-87	90	177	-5.74	NA	-	.0325
19	HT-1 Cover + 7 layers Al-Mylar laminate			Top Right (#2)	436	293	91.7	201	1.48		1.493-1.626 1.559(avg)	.00736
19	HT-1 Cover + 7 layers Al-Mylar laminate	39.9 / 39.7	0.50	Top Right	-	-96	90	186	-.37	.0126	-	.00199
20	H-S Al woven cover + 7 layers Al-Mylar with woven dacron scrim			Top Left (#1)	412	349	92.7	256	6.83		2.420-2.682 2.55(avg)	.0267
20	H-S Al woven Cover ± 7 layers Al-Mylar with woven dacron scrim	33.1 / 32.5	1.82	Top Left	-	-76	91	167	-.804	.0220	-	.00481

TABLE 7

TEST RESULTS, FOURTH DAY

DATE: 16 APRIL 1963

SAMPLE NUMBER	SAMPLE DESCRIPTION	WEIGHT BEFORE / WEIGHT AFTER GRAMS	WEIGHT LOSS %	TEST POSITION	HEAT ± 5% $FLUX_{ses}$ BTU/HR-Ft^2	SURFACE TEMP °F	BACK PLATE TEMP. °F	△ T SURFACE BACK PLATE °F	Q HEAT FLOW BTU/HR-Ft^2	ϵ TEST	α/ϵ TEST	J BTU/HR-Ft^2-°R
21	Rayon Cover + Polyurethane +Nylon Treco (B.F. Goodrich)			Top Right (#2)	436	156	93.6	62.4	21.0		.616-.681 .648(avg)	.3365
21	Rayon Cover + Polyurethane + Nylon Treco (B.F. Goodrich)	44.1 / 43.54	1.27	Top Right	-	-99	93	192	-17.65	.603	-	.0919
22	7 layers Al-Mylar laminated to Nylon Tulle Spacer			Middle Left (#3)	490	303	93.6	209.4	11.7		2.328-2.578 2.453(avg)	.0559
22	7 layers Al-Mylar laminated to Nylon Tulle Spacer	25.2 / 22.59	10.37	Middle Left	-	-98	93.7	191.7	-.55	.01913	-	.002865
24	7 layers Al-Mylar,Spot laminated, Dacron Scrim separator			Middle Right (#4)	446	341	93.6	247.4	4.24		1.650-1.823 1.736(avg)	.01717
24	7 layers Al-Mylar,Spot laminated. Dacron Scrim. separator	33.45 / 32.83	1.85	Middle Right	-	-151	93.7	244.7	-.895	.0604	-	.00366
25	Al-Dacron Cover + 7 layers NRC-2			Lower Right (#6)	404	315	94	221	2.69		2.191-2.419 2.305(avg)	.01218
25	Al-Dacron Cover + 7 layers NRC-2	42.52 / 40.19	5.48	Lower Right	-	-103	94.5	197.5	-.24	.00885	-	.001216
27	Project Mercury Suit Material (B.F. Goodrich)			Top Left (#1)	410	138	95	43	23.80		2.215-2.455 2.335(avg)	.554
27	Project Mercury Suit Material (B.F. Goodrich)	50.18 / 42.72	14.87	Top Left	-	37	94.5	57.5	-7.10	.0325	-	.1235
36	ILC Suit Al-HT-1 + Nylon + Nylon impregnated with neoprene			Lower Left (#5)	383	161	93	68	18.10		1.492-1.620 1.556(avg)	.266
36	ILC Suit Al-HT-1 + Nylon + Nylon impregnated with neoprene	52.9 / 50.07	5.35	Lower Left	-	31.5	93	61.5	-5.26	.0529	-	.0855

71

TABLE 8

PREDICTED EQUILIBRIUM CONDITIONS FOR VARIOUS SAMPLE MATERIALS

MISSION-ENVIRONMENT	α/ϵ SOLAR & ALBEDO	α/ϵ PLANET RADIATION	SURFACE EQUILIBRIUM TEMPERATURE °F	HEAT FLOW BTU/HR-Ft^2	MATERIAL SAMPLE
Earth Orbit Maximum Radiation	2.06 (avg)	1.0	222	+1.78	HT-1+NRC-2 based on avg. test values for Samples 3, 4, 11
	2.335	1.0	110	+11.06	Project Mercury Suit, Sample 27
	.648	1.0	80	-3.365	Rayon-Polyurethane Nylon, Sample 21
	1.787	1.0	212	+1.48	Al-Mylar-Alodine NRC-2, Sample 1
	2.331	1.0	218	+1.05	Al-Mylar-Al-Fil , Sample 12
	1.559	1.0	191	+.744	Al-Mylar laminate, Sample 19
	1.64	1.0	200	+ .660	Al-Polypropylene laminate, Sample 1
Earth Orbit Minimum Radiation	-	1.0	-50	- .274	HT-1 + NRC-2, based on avg. test values for Samples 3, 4, 11
	-	1.0	70	-2.47	Project Mercury Suit, Sample 27
	-	1.0	-45	-12.4	Rayon-Polyurethane Nylon, Sample 21
	-	1.0	-52	-.353	Al-Mylar, Alodine + NRC-2, Sample 17

MISSION-ENVIRONMENT	α/ϵ SOLAR & ALBEDO	α/ϵ PLANET RADIATION	SURFACE EQUILIBRIUM TEMPERATURE °F	HEAT FLOW BTU/HR-Ft^2	MATERIAL SAMPLE
Earth Orbit Minimum Radiation	-	1.0	-58	-.0595	Al-Mylar, Al-Film Sample 12
	-	1.0	-40	-.258	Al-Mylar laminate, Sample 19
	-	1.0	-45	-.204	Al-Polpropylene laminate, Sample 15
Lunar Orbit Maximum Radiation	2.06 (avg)	1.0	229	+1.88	HT-1 + NRC-2, based on avg. test values for Samples 3, 4, 11
	2.335	1.0	110	+11.08	Project Mercury Suit, Sample 27
	.648	1.0	160	+23.6	Rayon-Polyurethane Nylon, Sample 21
	1.787	1.0	230	+1.69	Al-Mylar, Alodine + NRC-2, Sample 17
	2.331	1.0	219	+1.055	Al-Mylar-Al-Film, Sample 12
	1.559	1.0	220	+.956	Al-Mylar laminate, Sample 19
	1.64	1.0	222	+.792	Al-Polypropylene laminate, Sample 15
Lunar Orbit Minimum Radiation	-	-	-108	-.386	HT4 + NRC-2 based on avg. test values for Samples 3, 4, 11

MISSION-ENVIRONMENT	α/ϵ SOLAR & ALBEDO	α/ϵ PLANET RADIATION	SURFACE EQUILIBRIUM TEMPERATURE °F	HEAT FLOW BTU/HR-Ft^2	MATERIAL SAMPLE
Lunar Orbit Minimum Radiation	-	-	60	-3.71	Project Mercury Suit, Sample 27
	-	-	-101	-9.29	Rayon-Polyurethane Nylon, Sample 21
	-	-	-120	-.523	Al-Mylar, Alodine + NRC-2, Sample 17
	-	-	-135	-.0905	Al-Mylar, Al-Film, Sample 12
	-	-	-100	-.378	Al-Mylar laminate, Sample 19
	-	-	-105	-.294	Al-Polypropylene laminate, Sample 1
Lunar Surface Maximum Radiation	2.06 (avg)	1.0	152	+.836	HT-1 + NRC-2, based on avg. test values for Samples 3, 4, 11
	2.335	1.0	100	+5.54	Project Mercury Suit, Sample 27
	.648	1.0	80	-3.365	Rayon-Polyurethane Nylon, Sample 21
	1.787	1.0	159	+.835	Al-Mylar Alodine + NRC-2, Sample 17
	2.331	1.0	158	+.556	Al-Mylar, Al-Film, Sample 12
	1.559	1.0	140	+.368	Al-Mylar laminate, Sample 19

MISSION-ENVIRONMENT	α/ϵ SOLAR & ALBEDO	α/ϵ PLANET RADIATION	SURFACE EQUILIBRIUM TEMPERATURE °F	HEAT FLOW BTU/HR-Ft^2	MATERIAL SAMPLE
Lunar Surface Maximum Radiation	1.64	1.0	148	+.348	Al-Polypropylene laminate, Sample 15
Lunar Surface Minimum Radiation	See Lunar Orbit - Minimum Radiation				

T_{inside} = 90°F

\+ = Heat Flow In

\- = Heat Flow Out

TABLE 9

COMPARISON OF MOST SUITABLE COVERALL MATERIALS

SAMPLE	SAMPLE PREFERENCE	MISSION	HEAT FLOW IN BTU/HR-Ft^2	HEAT FLOW OUT BTU/HR-Ft^2	Δ Q BTU/HR-Ft^2	N_{Phot} $\frac{\text{BTU-LB}}{\text{HR-Ft}^2\text{-}^\circ\text{R}}$	N_{Pcold} $\frac{\text{BTU-LB}}{\text{HR-Ft}^2\text{-}^\circ\text{R}}$
HT-1 + 7 Al-Polypropylene laminate with dacron spacers (#15)	1	Earth Orbit	0.660	0.204	0.864	.00053	.0001334
		Lunar Orbit	0.792	0.294	1.086	.00053	.0001334
		Lunar Surface	0.348	0.294	0.642	.00053	.0001334
HT-1 + 7 Al-Mylar laminate with dacron Spacers (#19)	2	Earth Orbit	0.744	0.258	1.002	.000652	.0001741
		Lunar Orbit	0.956	0.378	1.334	.000652	.0001741
		Lunar Surface	0.368	0.378	0.746	.000652	.0001741
HT-1 + 7 Al-Mylar-Al Film with dacron spacers (#12)	3	Earth Orbit	1.05	0.06	1.11	.000515	.0000254
		Lunar Orbit	1.055	0.0905	1.1455	.000515	.0000254
		Lunar Surface	0.556	0.0905	0.6465	.000515	.0000254

SAMPLE	SAMPLE PREFERENCE	MISSION	HEAT FLOW IN BTU/HR-Ft^2	HEAT FLOW OUT BTU/HR-Ft^2	ΔQ BTU/HR-Ft^2	N_{Phot} BTU-LB / HR-Ft^2-$^\circ$R	N_{Pcold} BTU-LB / HR-Ft^2-$^\circ$R
HT-1 + 7 MRC-2 with dacron spacers (based on avg. values for Samples 3, 4, 11	4	Earth Orbit	1.78	0.274	2.054	.00087	.0001266
		Lunar Orbit	1.88	0.386	2.266	.00087	.0001266
		Lunar Surface	0.836	0.386	1.222	.00087	.0001266

$T_{inside} = 90^\circ F$

APPENDIX

THE EFFECT OF EDGE LOSSES ON THERMAL-FLOW MEASUREMENTS

PROBLEM

The edge effects on the steady state heat flow measurements in superinsulation was analyzed to determine the magnitude of any errors caused by these edge effects. The analysis conducted is summarized in the following paragraphs.

ANALYSIS

The incident energy on the specimen which is absorbed is conducted into the surface. Now assume that the engery leaving the back side of the specimen is less than that which was captured; normally, the difference is recognized as heat stored by a material to raise its temperature. But in steady state operations, temperature changes have, by definition, ceased; the difference has become spanwise or lateral conduction, a built-in testing error.

A steady state analysis of Figure 1 describes the surface temperature distribution along the X-axis.

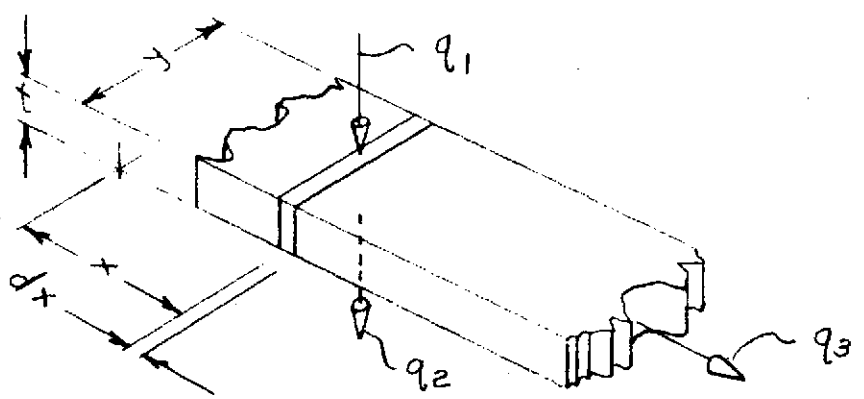

FIGURE 1

$$(1)\quad dq_3 = \frac{\alpha}{\epsilon}\, q_i\, dA = \frac{\alpha}{\epsilon}\, q_i\, y\, dx$$

which after integrating is

$$q_3 = \frac{\alpha}{\epsilon}\, q_i\, y\, x$$

$$(2)\quad -k_3 t \frac{dT}{dx} = q_3 = \frac{\alpha}{\epsilon}\, q_i\, y\, x$$

$$-dT = \frac{\alpha}{\epsilon}\, \frac{q_i}{kt}\, x\, dx$$

$$\int_{T_1}^{T_3} -dT = \int_0^x \frac{\alpha}{\epsilon}\, \frac{q_i}{kt}\, x\, dx$$

$$-T \Big]_{T_1}^{T_3} = \frac{\alpha}{\epsilon}\, \frac{q_i\, x^2}{2kt} \Big]_0^x$$

$$T_1 - T_3 = \frac{\alpha}{\epsilon}\, \frac{q_i\, x^2}{2kt}$$

Therefore, the spanwise temperature distribution is parabolic.

Using specimen 10 as an example, the lateral heat flow from a 3" x 3" thermopile was determined as follows:

Specimen 10 consists of:

7 layers, 1/4 mil mylar with .001 mil aluminum on one side

$K_{mylar} = 1.92 \frac{BTU\ IN}{HR\ Ft^2\ ^oR}$

$K_{Al} = 1400 \frac{BTU\ IN}{HT\ Ft^2\ ^oR}$

and

6 spacers, 1 mil dacron matte (15% solid)

$K_{dacron} = 1.08 \frac{BTU\ IN}{HR\ Ft^2\ ^oR}$

The effective U from one side will be:

$$\frac{1}{U_1} = \frac{12}{1.92(.00175).25} + \frac{12}{1.08(.006)(.15).25} + \frac{12}{1400(.000007).25}$$

$$U_1 = 1.43(10^{-5}) \frac{BTU}{HR\ ^oR}$$

So that for one side

$$q_3 = U_1 \left(\frac{dT}{dx}\right)_{x = 1.5} = 1.458(10^{-5}) \left(\frac{dT}{dx}\right)_{x = 1.5}$$

For three sides

$$q_3 = 4.37(10^{-5}) \left(\frac{dT}{dx}\right)_{x = 1.5}$$

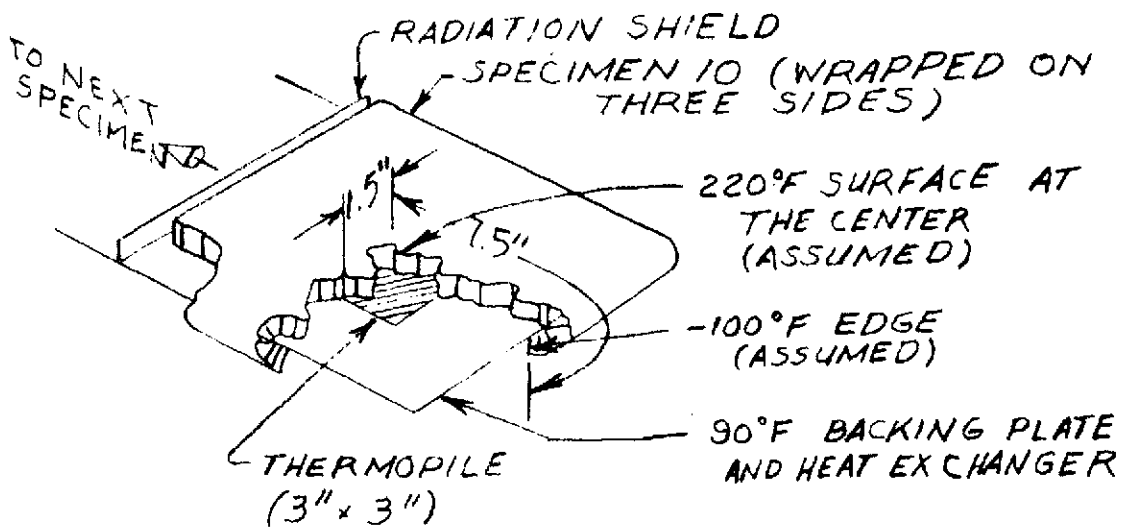

FIGURE 2

Using the parabolic temperature distribution and values indicated on Figure 2,

$$T_{center(avarage)} - T_{edge} = \frac{CX^2}{2}$$

$$\left(\frac{220 + 90}{2}\right) - (-100) = C\,\frac{(7.5)^2}{2}$$

$$C = 9.08\ \frac{^oF}{in^2}$$

$$\left(\frac{dT}{dx}\right)_{x = 1.5} = CX = 13.62\ \frac{^oF}{in}$$

The spanwise loss at the thermopile edge is

$$q_3 = 4.37(10^{-5})\ \ 13.62 = .000595\ \frac{BTU}{HR}$$

CONCLUSION

This lateral conduction (.000595 $\frac{BTU}{HR}$) represents 1.8% of the heat flow entering sample number 10 (thermopile area) and is therefore negligible.